2015

Resistive Pulse study of Vesicles and Liposomes

Yuqing Lin
University of Central Florida

RESISTIVE PULSE STUDY OF VESICLES AND LIPOSOMES

by

YUQING LIN
B.S. Beijing Normal University, 2008
M.S. University of Central Florida, 2010

A dissertation submitted in partial fulfillment of the requirements
for the degree of Doctor of Philosophy
in the Department of Physics
in the College of Science
at the University of Central Florida
Orlando, Florida

Summer Term
2015

Major Professor: Lee Chow

ABSTRACT

In this work, the properties of the liposomes, the artificially created vesicles by various methods, are explored by a resistive pulse method using micropipettes. The fact that vesicles are fundamental in the wide range of functionalities they fulfill as organelles strengthen the desire of understanding the properties of them. The motivation of this work comes from the significant roles that liposomes play in the development of targeted drug delivery systems. Among other significant variables, the size of liposomes is found to be one of the dominating parameters in liposome based drug delivery, and the correlation between liposome size and delivery efficiency is discussed. To help improving the size evaluation ability, a few mainstream methods for liposome size detection and measurements are reviewed. As a reliable and accessible alternative method for liposomes detection, the resistive pulse method is introduced and the measurement on liposomes size change upon pH gradient was performed using this method. With our current liposome composition, we found the size increases as environmental pH increases. Further investigation is performed with vesicular pH=6, 7, and 8, respectively. Lastly, the stability of the small unilamellar vesicles (SUV) was studied via resistive pulse method, by monitoring the size change of 50nm liposomes as function of time. A significant size change in freshly prepared 50nm liposomes is recorded. This information will provide invaluable knowledge for targeting tumor with tight tissues, where small size liposomes are needed.

To all the challenges in physics.

ACKNOWLEDGMENTS

First and foremost, I would like to thank my professor, Dr Lee Chow for his guidance and help throughout my graduate school years. Always kind, wise, and ready to help, Dr Chow offers me his mentorship and friendship, which I will forever treasure. I also would like to thank Dr Tatulian, Dr Shulte and Dr Yuan for all the help and taking time to be on my committee. A significant part of the research is performed in Dr Tatulian's lab with tremendous help and guidance from Dr Tatulian and Dr Kathleen Nemec. Dr Tatulian not only let me use the equipment in the lab but also providing insightful ideas and literatures. Dr Nemec is such a caring, nice and knowledgeable scholar, she generously shares her sample, her expertise, and her kind heart with me. I will always remember the time we spent together doing experiments and talking about biology, physics, and Asian history while having a Chinese/Japanese fusion lunch. Also, the undergraduate research assistant, Ms Joselyn Morales, offered me great help with the experiments too. I wish her all the best in her academic pursuit in graduate school. Dr Tatulian's lab will always have a special place in my memory as it is a fruitful and productive lab for research, and a heart-warming place for everyone who have worked there. Many thanks to everyone who help and support me at UCF.

TABLE OF CONTENTS

LIST OF FIGURES

LIST OF TABLES

CHAPTER 1 INTRODUCTION

Vesicles: Function And Properties

Vesicles are a commonly found organelle in cells, formed by lipid bilayer membrane structure in aqueous environment. Figure 1 shows the structure of vesicles are self-constructed, the heads of the lipid group, which are hydrophilic, are at the inner and outer surface of the membrane, while the hydrophobic tails are enclosed inside.

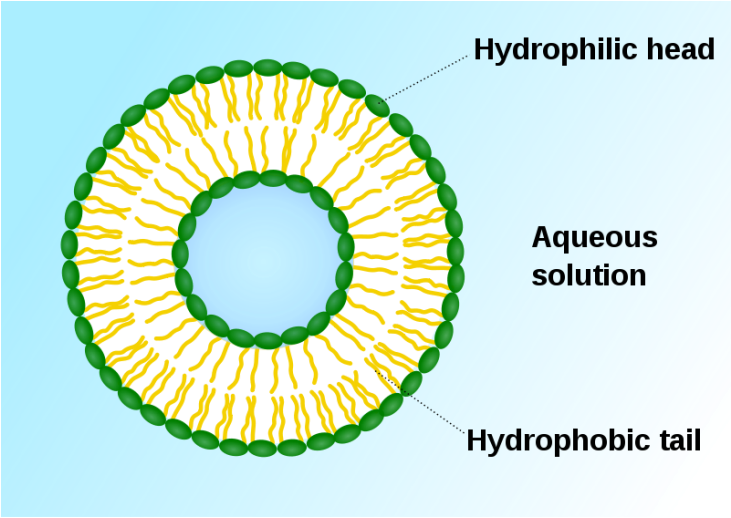

Figure 1 The lipid bilayer structure of vesicles

http://en.wikipedia.org/wiki/Vesicle_%28biology_and_chemistry%29

The formation of vesicles are various. In natural formation of vesicles includes exocytosis and endocytosis, these processes allow vesicle to enclose particles or molecules within the cytoplasm, outside of cytoplasm, and across cytoplasm. The

artificial fabricated vesicles are given a specific name, liposomes, which have the same transportation feature like their natural counterpart, but with a wide range of tunable variables which would be of great interest and importance.

Another way to categorize vesicles is by their size and the number of phospholipid bilayer they have [1, 2]. As shown by Figure 2, vesicles with multiple bilayers can be as large as 500nm to 5000nm, while LUV, or large unilamellar vesicles, range from around 100nm to 500nm; and SUV, or small unilamellar vesicles, have a size of 100nm to as low as 20nm. These unilamellar vesicles contain only one lipid bilayer[3], as shown in Figure 3. The liposomes, though artificial prepared, followed the same categorization method.

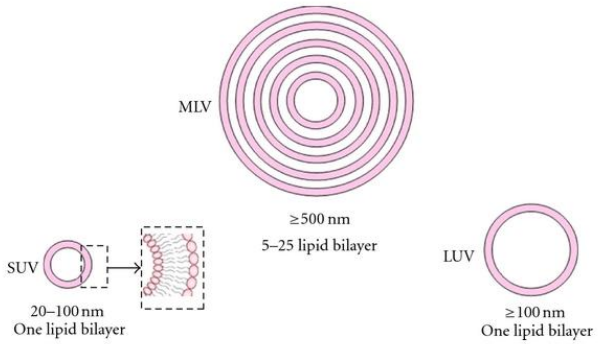

Figure 2 Vesicles of different size and number of lipid bilayers, Reprinted from F. Yang, C. Jin, Y. Jiang, J. Li, Y. Di, Q. Ni, D. Fu, Liposome based delivery systems in pancreatic cancer treatment: From bench to bedside, Cancer Treatment Reviews, 37 (2011) 633-642, with permission from Elsevier

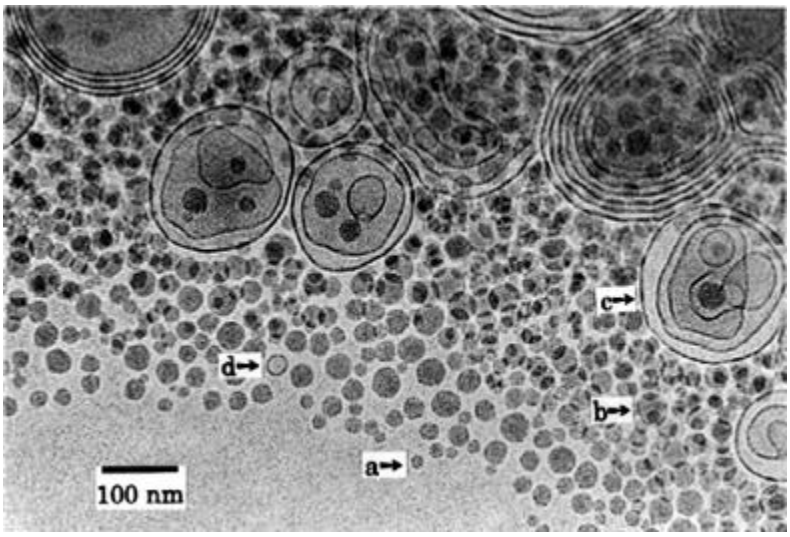

Figure 3 Cryo-TEM of various vesicles. (a) poly particles (b) overlapping particles (c) multilamellar vesicles (d) unilamellar vesicles

Reproduced from F. Yan, J. Texter, Capturing nanoscopic length scales and structures by polymerization in microemulsions, Soft Matter, 2 (2006) 109-118 with permission of The Royal Society of Chemistry

The bilayer enclosed structure give vesicles the possibility to fulfill many functions. For example, the separation of what is inside the vesicles from the cytosol or any other environment liquid makes vesicles ideal to organize cellular substances like Golgi apparatus, transport or store particles or molecules, or serve as chemical reaction chamber[4].

An example: Synaptic vesicles

A great example to demonstrate the function of vesicles is nerve impulse propagation process. Neurotransmitters, which are stored in synaptic vesicles of the neuron, are

transported and released under the excitation voltage along calcium channel from transmitting neuron to receiving neuron. The place where neurotransmitter move between the two participating neurons is called bouton. Depends on the functions and locations in neuron bouton, there are three groups of synaptic vesicles, shown as Figure 4.

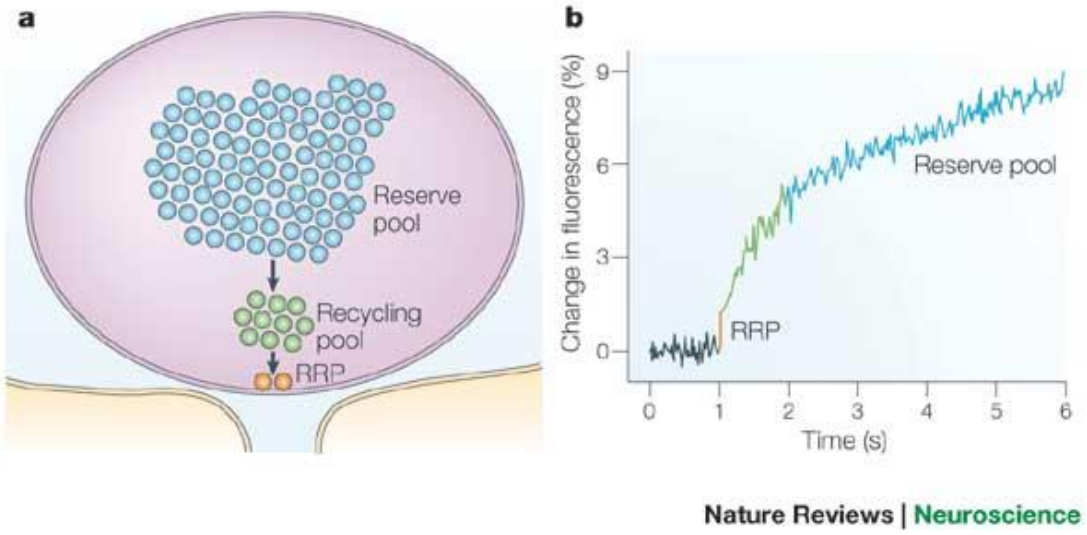

Figure 4 The three pool model. (a) The reserve pool consists about 80 to 90% of the total vesicle count, while the recycle pool has about 10 to 15%. The readily release pool has about 1%. (b) The release of three vesicle pools. Reprinted by permission from Macmillan Publishers Ltd: S.O. Rizzoli, W.J. Betz, Synaptic vesicle pools, Nat Rev Neurosci, 6 (2005) 57-69

Table 1 Characteristics of the vesicle pools, Reprinted by permission from Macmillan Publishers Ltd: S.O. Rizzoli, W.J. Betz, Synaptic vesicle pools, Nat Rev Neurosci, 6 (2005) 57-69

Table 1 | **Characteristics of the vesicle pools**

Pool	Readily releasable pool (RRP)	Recycling pool	Reserve pool
Size (% of all vesicles)	~1–2%	~10–20%	~80–90%
Location	Docked	Scattered	Scattered (bulk of vesicle cluster)
Released within	<1 second	A few seconds	Tens of seconds, minutes
Recycling	Fast (seconds)	Fast (seconds)	Slow (minutes)
Mixing with other pools	Fast mixing with recycling vesicles	Slow mixing with reserve	Slow mixing with other vesicles
Mobility in resting terminals	None — docked	High	Low (high in bipolar cells)

The first pool is the readily releasable pool, which is docked to the neuron membrane. This pool will response upon incoming pulse, immediately release neurotransmitter. Due to its relatively small size, the readily releasable pool doesn't last long. Next is the recycling pool which is located in the vicinity of membrane. It is larger and response slower than the readily release pool. The stimulation drives the vesicles in the recycling pool to release at a rate no greater than vesicle formation rate, while the vesicles in readily release pool release much faster than formation. The last is the reservation pool, where the majority of the vesicles exist. The release in this pool normally happen under heavy stimulation, when the vesicles from readily release pool and recycle pool are

mostly released[5], as shown in Table 1. A typical release rate is about 130 vesicles per bouton over 10 minutes, which is equal to 0.2 Hz[6].

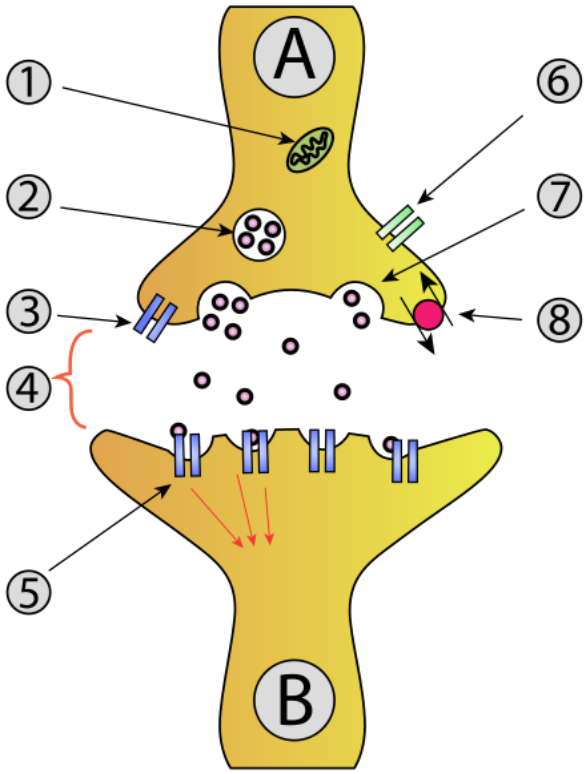

Figure 5 Transmitting neuron A to receiving neuron B. 1.Mitochondria 2.Synaptic vesicles with neurotransmitters 3.Autoreceptor 4.Synapse, where synaptic vesicles release neurotransmitter 5. Receptors activated by neurotransmitter 6.Calcium channel 7.Synaptic vesicles exocytosis 8. Recaptured neurotransmitter

http://en.wikipedia.org/wiki/Synaptic_vesicle#cite_note-Rizzoli_Betz_2005-22

The synaptic vesicle cycle, starts from the initial trafficking of synaptic vesicles to synapse. Once there, with the help of neurotransmitter transporter and a proton pump, the transmitter are loaded. The synaptic vesicles are then docked in the vicinity of

releasing site. Then a process called priming is in place to make the vesicles ready to fuse fast when the calcium gradient is present. After the preparation, the vesicles can began fusion rapidly in response to incoming pulse[7]. Then the exocytosis and endocytosis process will begin, as illustrated in Figure 5.

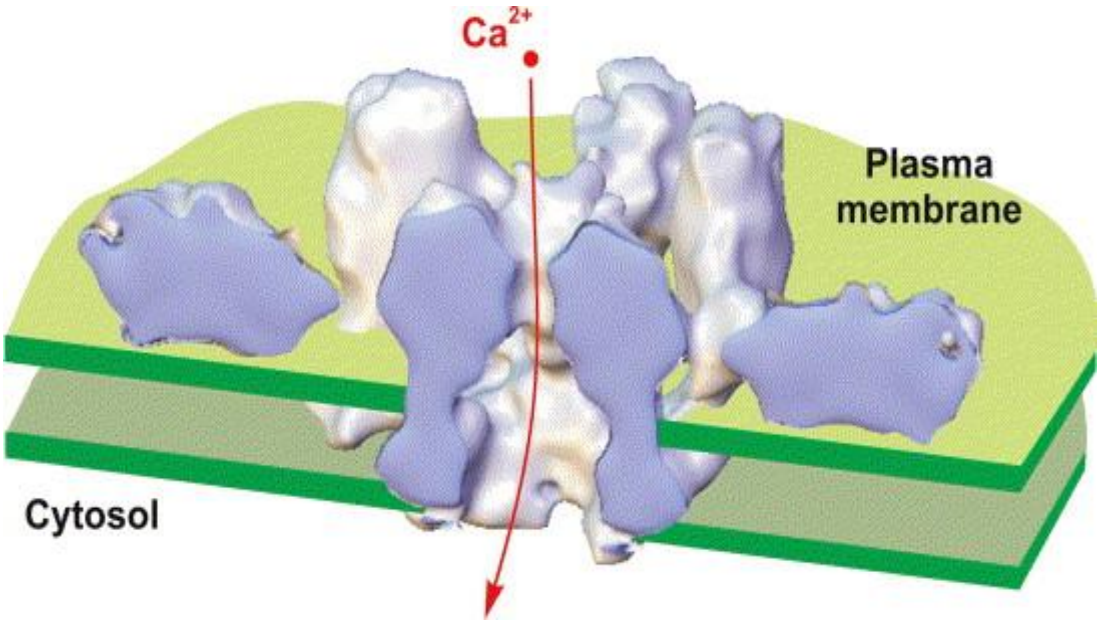

Figure 6 a model of αLTX pore in the membrane bilayer structure. Reprinted from Y.A. Ushkaryov, K.E. Volynski, A.C. Ashton, The multiple actions of black widow spider toxins and their selective use in neurosecretion studies, Toxicon, 43 (2004) 527-542. With permission from Elsevier

Due to the vital role vesicles play in the basic function of neurons, it is natural to conclude that if vesicles malfunctioned or are damaged, the corresponding syndrome will surface. For example, batrachotoxin, a neurotoxin, will permanently bind to the sodium ion channel of vesicles and break it. The osmosis gradient will then damage the synaptic vesicles and therefore endanger the neuron system [8]. Another similar

example is alpha-latrotoxin, from the famous black widow spider venom. As shown in Figure 6, alpha-latrotoxin will form pores which are permeable to calcium ions and neurotransmitters. This will cause significant calcium ion inflow and neurotransmitter leakage, therefore severely damage the neuron system[9].

In medical research, it is suggested a strong correlation between the misbehavior of cell vesicles and some of the most medical challenging disease, like diabetes, Alzheimer's disease. Three researchers, james Rothman, Randy Schekman, Thomas Sudhof, are awarded with 2013 Nobel Prize in Physiology or Medicine, for their discovery of the role which vesicles play in the above mentioned disease.

CHAPTER 2 LIPOSOME SIZE AND DRUG DELIVERY

Liposomes: Drug Delivery Vehicle

The rapid development of nanotechnology recently has generated a tremendous interest in new method of disease treatment, especially in cancer. Nanotechnology created structures, such as polymer micelles, carbon nanotubes, nanoparticles, and liposomes haven been heavily involved in the drug delivery carrier research [2]. Among them, liposome based drug delivery system demonstrated superb maturity and huge potential, since the encapsulation structure is the key to reduce the complexity and difficulty to target tumor cell while reducing side effect, especially for chemotherapeutic drugs that might be harmful, sometimes even cytotoxic, to normal cells. The potential of liposomal drug delivery systems are greatly appreciated by the pharmaceutical industry and gained increasing approval from FDA, the Food and Drug Administration of USA. A summary[10] of the currently available liposomal drugs are shown in Table 2, and currently under trial liposomal drugs are shown in Table 3.

Table 2 Liposomal drugs on the market. Reproduced from H.-I. Chang, M.-K. Yeh, Clinical development of liposome-based drugs: formulation, characterization, and therapeutic efficacy, International Journal of Nanomedicine, 7 (2012) 49-60, Reproduced with permission of DOVE Medical Press in the format Republish in a thesis/dissertation via Copyright Clearance Center.

Table 1 Liposome-based drugs on market

Product name	Route of injection	Drug	Particle type/size	Drug form/Storage time	Lipid composition	Approved indication
Ambisome	Intravenous	Amphotericin B	Liposome	Powder/36 months	HSPC, DSPG, cholesterol, and amphoteracin B (2:0.8:1:0.4 molar ratio)	Sever fungal infections
Abelcet	Intravenous	Amphotericin B	Lipid complex	Suspension/24 months	DMPC and DMPG (7:3 molar ratio)	Sever fungal infections
Amphotec	Intravenous	Amphotericin B	Lipid complex	Powder/24 months	Cholesteryl sulfate	Sever fungal infections
DaunoXome	Intravenous	Daunorubicin	Liposome	Emulsion/12 months	DSPC and cholesterol (2:1 molar ratio)	Blood tumors
Doxil	Intravenous	Doxorubicin	PEGylated liposome	Suspension/20 months	HSPC, cholesterol, and PEG 2000-DSPE (56:39:5 molar ratio)	Kaposi's sarcoma, Ovarian/breast cancer
Lipo-dox	Intravenous	Doxorubicin	PEGylated liposome	Suspension/36 months	DSPC, cholesterol, and PEG 2000-DSPE (56:39:5 molar ratio)	Kaposi's sarcoma, ovarian/breast cancer
Myocet	Intravenous	Doxorubicin	Liposome	Powder/18 months	EPC and cholesterol (55:45 molar ratio)	Combination therapy with cyclophosphamide in metastatic breast cancer
Visudyne	Intravenous	Verteporfin	Liposome	Powder/48 months	EPG and DMPC (3:5 molar ratio)	Age-related molecular degerneration, pathologic myopia, ocular histoplasmosis
Depocyt	Spinal	Cytarabine	Liposome	Suspension/18 months	Cholesterol, Triolein, DOPC, and DPPG (11:1:7:1 molar ratio)	Neoplastic meningitis and lymphomatous meningitis
DepoDur	Epidural	Morphine sulfate	Liposome	Suspension/24 months	Cholesterol, Triolein, DOPC, and DPPG (11:1:7:1 molar ratio)	Pain management
Epaxal	Intramuscular	Inactivated hepatitis A virus (strain RG-SB)	Liposome	Suspension/36 months	DOPC and DOPE	Hepatitis A
Inflexal V	Intramuscular	Inactivated hemaglutinine of Influenza virus strains A and B	Liposome	Suspension/12 months	DOPC and DOPE	Influenza

Table 3 Liposomal drugs on clinic trials Reproduced from H.-I. Chang, M.-K. Yeh, Clinical development of liposome-based drugs: formulation, characterization, and therapeutic efficacy, International Journal of Nanomedicine, 7 (2012) 49-60, Reproduced with permission of DOVE Medical Press in the format Republish in a thesis/dissertation via Copyright Clearance Center.

Table 2 Liposome-based drugs in clinical trials

Product name	Route of injection	Drug	Lipid composition	Approved indication	Trial phase
LEP-ETU (powder/12 months)	Intravenous	Paclitaxel	DOPC, cholesterol, and cardiolipin (90:5:5 molar ratio)	Ovarian, breast, and lung cancers	Phase I/II
LEM-ETU	Intravenous	Mitoxantrone	DOPC, cholesterol, and cardiolipin in 90:5:5 molar ratio	Leukemia, breast, stomach, liver, ovarian cancers	Phase I
EndoTAG-1 (powder/24 months)	Intravenous	Paclitaxel	DOTAP, DOPC, and paclitaxel (50:47:3 molar ratio)	Anti-angiogenic properties, breast cancer, pancreatic caner	Phase II
Arikace	Portable aerosol delivery	Amikacin	DPPC and cholesterol	Lung infection	Phase III
Marqibo	Intravenous	Vincristine	Cholesterol and egg sphingomyelin (45:55 molar ratio)	Metastatic malignant uveal melanoma	Phase III
ThermoDox	Intravenous	Doxorubicin	DPPC, MSPC, and PEG 2000-DSPE (90:10:4 molar ratio)	Non-resectable hepatocellular carcinoma	Phase III
Atragen	Intravenous	Tretinoin	DMPC and soybean oil	Acute promyelocytic leukemia, hormone-refractory prostate cancer	Phase II
T4N5 liposome lotion	Topical	Bacteriophage T4 endonuclease 5	Unknown	Xeroderma pigmentosum.	Phase III
Liposomal Grb-2	Intravenous	*Grb2* antisense oligodeoxynucleotide	Unknown	Acute myeloid leukemia, chronic myelogenous leukemia, acute lymphoblastic leukemia	Phase I
Nyotran	Intravenous	Nystatin	DMPC, DMPG, and cholesterol	Systemic fungal infections	Phase I/II
LE-SN38	Intravenous	SN-38, the active metabolite of irinotecan	DOPC, cholesterol, and cardiolipin	Metastatic colorectal cancer	Phase I/II
Aroplatin	Intrapleural	Cisplatin analog (L-NDDP)	DMPC and DMPG	Metastatic colorectal carcinoma	Phase II
Liprostin	Intravenous	Prostaglandin E1	Unknown	Peripheral vascular disease	Phase II/III
Stimuvax	Subcutaneous	BLP25 lipopeptide (MUC1-targeted peptide)	Monophosphoryl lipid A, cholesterol, DMPG, and DPPC	Cancer vaccine for multiple myeloma developed encephalitis	Phase III
SPI-077	Intravenous	Cisplatin	SHPC, cholesterol, and DSPE-PEG	Head and neck cancer, lung cancer	Phase I/II
Lipoplatin (suspension/36 months)	Intravenous	Cisplatin	SPC, DPPG, cholesterol, and mPEG 2000-DSPE	Pancreatic cancer, head and neck cancer, mesothelioma, breast and gastric cancer, and non-squamous non-small-cell lung cancer	Phase III
S-CKD602	Intravenous	Camptothecin analog	DPSC and DSPE-PEG (95:5 molar ratio)	Recurrent or progressive carcinoma of the uterine cervix	Phase I/II
OSI-211	Intravenous	Lurtotecan	HSPC and cholesterol (2:1 molar ratio)	Ovarian cancer, head, and neck cancer	Phase II
INX-0125	Intravenous	Vinorelbine	Cholesterol and egg sphingomyelin (45:55 molar ratio)	Advanced solid tumors	Phase I
INX-0076	Intravenous	Topotecan	Cholesterol and egg sphingomyelin (45:55 molar ratio)	Advanced solid tumors	Phase I
Liposome-annamycin (powder)	Intravenous	Annamycin	DSPC, DSPG, and Tween	Acute lymphocytic leukemia	Phase I/II

The lipid bilayer of liposomes are made of nontoxic, bio-environment friendly phospholipids and cholesterol. The hydrophobic drugs are carried within the bilayer where the hydrophobic tails group of the phospholipids are, the hydrophilic drugs are enclosed inside the inner chamber formed by head group of phospholipids of the inner layer. This drug loading design minimized the contact from the drug before release, due to the high biocompatibility of phospholipids. The size of the liposomes are fully tunable, depends on the way of preparation and composition requirement. The diameter of the liposomes ranges from smaller than 50nm to as large as 1000nm. The versatile lipid bilayer can be also augmented with protein, peptide, or nanoparticles to help targeting the cancer cell or improve stability. Overall, the liposomes are excellent in biocompatibility and biodegradability, low toxicity and immunogenicity, while the tunable size and modifiable feature make it easy to enhance the targeting ability, in-vivo stability, and circulation time.

Correlation Between Liposome Size And Delivery Efficiency

Among all the variables that will affect the viability and efficiency of liposomal drug delivery, the size of liposome is getting increasingly recognized as an instrumental factor. [11] This is because the circulation time and residence time of liposomes in the blood vessel will be heavily influenced by particle size, along with the accumulation efficiency of liposomes at the vicinity of tumor tissue. Furthermore, the in vivo releasing mechanism of drugs which carried by liposomes will also depends on their size. Since

some of the antitumor drugs could be potentially toxic for the normal tissue, the size of the liposome becomes very crucial in delivery vehicle design.

In order for the antitumor drug to take effect, the liposomal vehicle needs to have the ability to transfer the drugs from blood through the wall of vein into the interstitial space of tumor. While the penetration of liposome through the vessel has been confirmed and well-studied [12], the accumulation of liposome, which is essential to achieve minimum amount of drug to be effective, is dominated by the composition and the size of liposomes. This process has put the size-efficiency investigation under the focus of pharmacokinetics and pharmacodynamics.

To better illustrate this, a test using tritium labeled liposomes on Yoshida sarcoma carrying rats were performed. After 24 hours the injected rats were killed and tumor uptake clearance is measured as a function of liposome size, ranging from 40 to 400nm.[11] The uptake rate difference at various sizes are significant, furthermore, at around 120nm an optimal uptake clearance is exhibited, clearly indicates the important role liposome size plays in drug delivery.

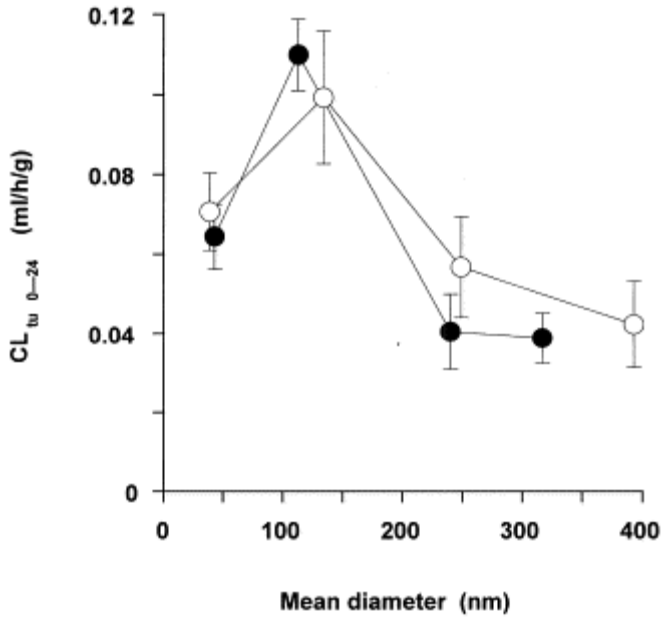

Figure 7 Tumor uptake clearance as function of liposome size. Reprinted from A. Nagayasu, K. Uchiyama, H. Kiwada, The size of liposomes: a factor which affects their targeting efficiency to tumors and therapeutic activity of liposomal antitumor drugs, Advanced drug delivery reviews, 40 (1999) 75-87, with permission from Elsevier

Size of the delivery vehicle is also of extreme importance in brain tumor treatment. The protective nature of the blood brain barrier prevent the penetration of drug to brain parenchyma, in particular, cerebral blood vessel has much tighter junctions compare to non-cerebral blood vessel, as illustrated in Figure 8. [13] Therefore as a tradeoff between loading capacity and permeability, the size of liposome need to be carefully planned.

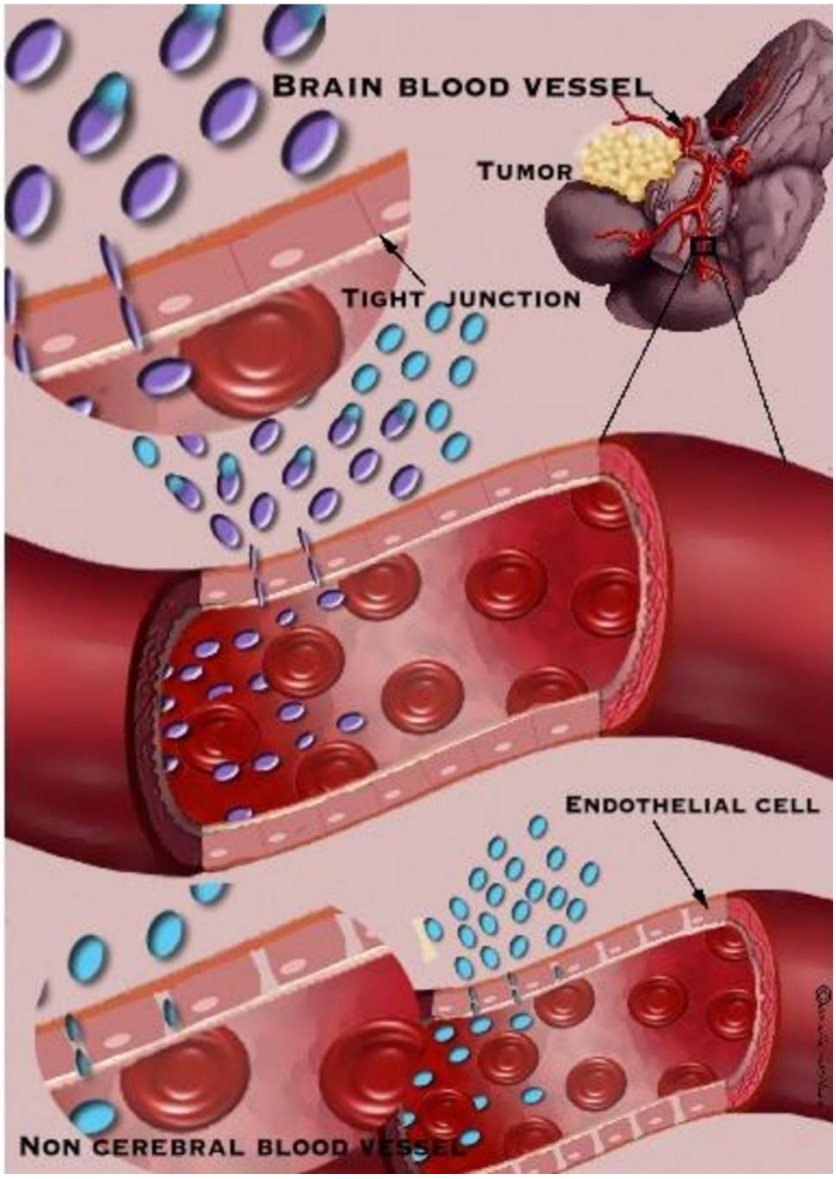

Figure 8 Comparison of cerebral blood vessel and non-cerebral blood vessel, Open access article with Creative Commons Attribution License http://www.vasculararcell.com/content/2/1/20

CHAPTER 3 SIZE DETECTION METHODS

Due to the critical role liposome size plays in drug delivery, a reliable and convenient method is needed to accurately measure the size. Here, a few established method, with their principles, set ups, applications and potential limitations, are briefly reviewed. The comparison of various size detection methods will provide insight on the advantage and therefore the motivation, of applying resistive pulse method as an alternative method for size detection. The details of resistive pulse method will be illustrated in the next chapter.

DLS (Dynamic Light Scattering)

Dynamic light scattering is among the most popular method for determining the size of particles in aqueous solution. Matured in the 60s of last century, DLS has achieved rapid and reliable detection of the diffusion coefficient of the particle, thus gaining the knowledge of particle size. The detection range can be from as small as 1 nm to micrometer level. Due to its rapid measurement, low sample consumption, and low sample damage, DLS has been widely used in bio-engineering, pharmaceutical industry, chemistry and microbiology.

The principle of DLS lies in the correlation of scattering light intensity and time. For example, if a particle is undergoing Brownian motion, the scattering light of it will be a fluctuated value instead of a constant, and the neighboring particles' scattering light,

also fluctuated, will interfere with it. The frequency of the fluctuation is depending on the size of particle and the relative angle between incident and scattered light. The smaller particles are, the more frequent fluctuations are. By analyzing this dependence, the particle size is obtained.

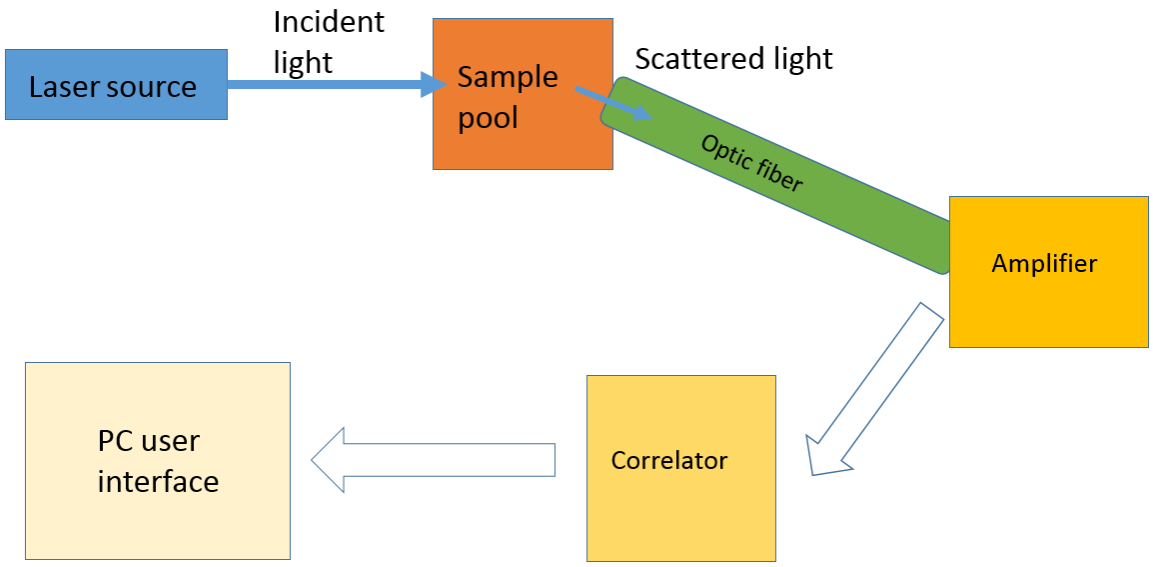

Figure 9 Dynamic light scattering experiment set up

As shown in Figure 9, a monochromic light beam, typically a laser, is shot on the sample pool, thus generating scattered light. Since the particles' diameters are usually below the wavelength, it will be a Rayleigh scattering where scattered light are in all directions. The autocorrelation function can be written as:

$$G(\tau) =< I(t)I(t+\tau) >= lim_{T\to\infty} \frac{1}{T}\int_0^T I(t)I(t+\tau)dt \quad (1)$$

Where *I* is the light intensity at a given time, thus the autocorrelation function, at monodisperse population, turns into:

$$G(\tau) = A[1 + \beta exp\,(-2\Gamma\tau)] \quad (2)$$

Where Γ is decay rate, which can be quantified as

$$\Gamma = q^2 D_T \quad (3)$$

With

$$q = \frac{4\pi n}{\lambda} Sin(\frac{\theta}{2}) \quad (4)$$

And

$$D_T = \frac{k_B T}{3\pi\eta d} \quad (5)$$

Where in equation 4 and 5, n is the refractive index of the solution, λ is the wavelength of the light, θ is the scattering angle, η is the viscosity of the solution, and d is the diameter of the particle. So when the computer calculates the correlation function, the diameter of the particles can be obtained.

Due to the rapid measurement speed and the reliable data repeatability, dynamic light scattering has become heavily involved in many applications: chemistry, medical research[14], food system[15], and fluid mechanics[16]. Also, dynamic light scattering

technique has been popular in liposome research, serving as a convenient tool for size measurement [17].

However, due to the algorithm of the correlation function calculation, the result of the size measurement has strong preference on the larger size, which makes the average size of DLS measurement shift to larger end[18]. Although DLS has been the mainstream instrument for size detection the demand of alternative methods is still present.

CryoTEM

CryoTEM is a technique of specialty TEM operation, with the sample of transmission electron microscopy is frozen, usually by liquid nitrogen. The most significant advantage of CryoTEM method is the high resolution provided from TEM, and the convenience of frozen sample, which makes it possible to be examined by TEM, therefore achieves higher resolution than environmental scanning electron microscope, or Wet SEM[18]. An example of CryoTEM size measurement can be seen in Figure 10.

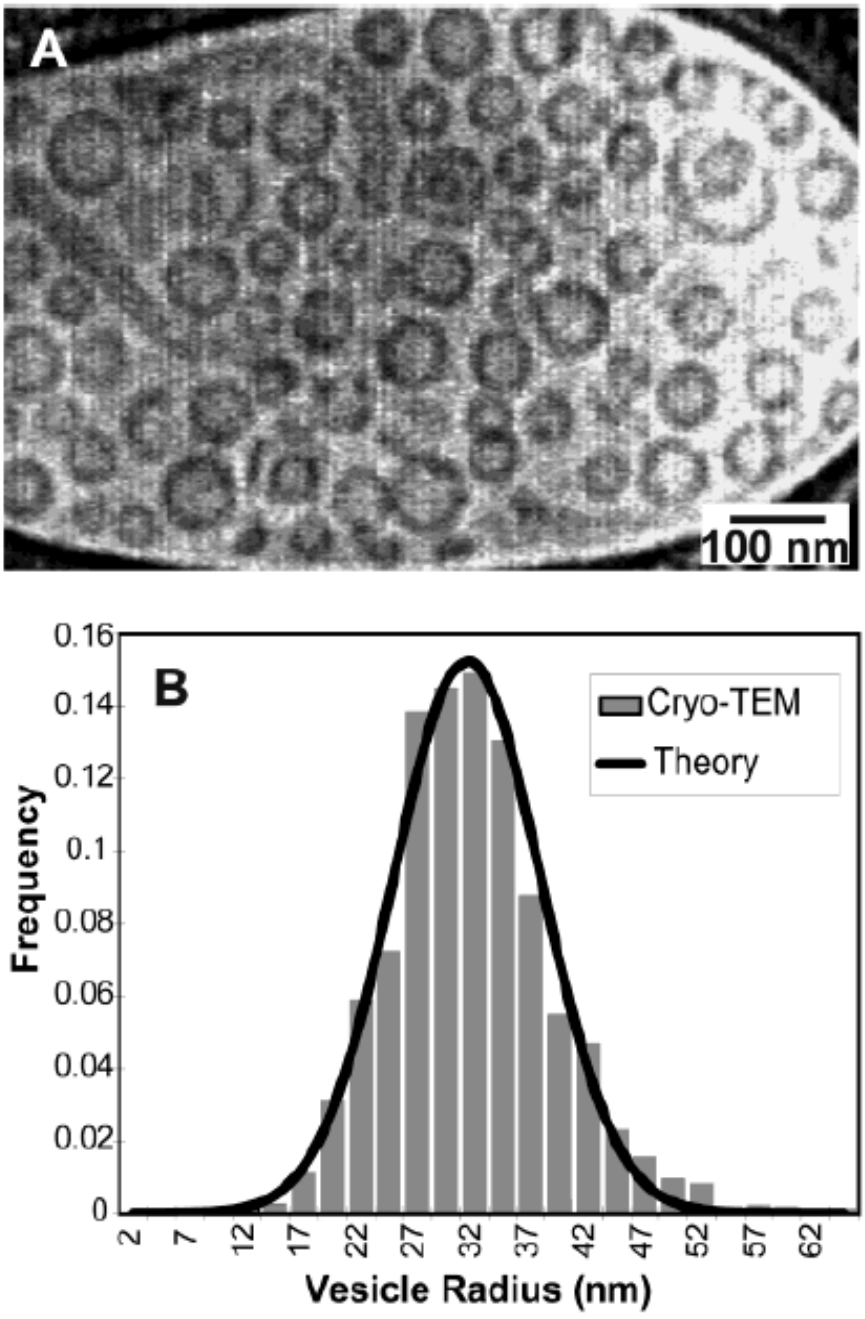

Figure 10 (a) CryoTEM image of vesicles (b) Size counting results by Image recognition software Image-Pro Plus 4.1 Reprinted with permission from B. Coldren, R. van Zanten, M.J. Mackel, J.A. Zasadzinski, H.-T. Jung, From Vesicle Size Distributions to Bilayer Elasticity via Cryo-Transmission and Freeze-Fracture Electron Microscopy, Langmuir, 19 (2003) 5632-5639, copyright 2003 American Chemistry Society

The result in CryoTEM is not a statistical ensemble like DLS, but a single particle resolution counting, with a clear visual of particle size and shape. However, CryoTEM, similar to DLS, has known problem with polydisperse size distribution sample[19]. The sample pool is small due to the limit of number of vesicles can be shown under TEM viewing screen, and the freezing process may potentially damage or alter the nature of sample.

Sonic Waves

The basic idea of this method is to apply AC voltage on the solution to generate a high frequency oscillation of the particles. The oscillation will create a sonic wave which propagating in the liquid, which eventually will be picked up by a piezoelectric sensor. By analyzing the delay between the phases of the sonic wave and the original electric wave signal, the information of the particle size can be obtained, since the larger particle will have larger inertia, and also experience more resistance from solution.

According to reference [20], the dynamic mobility μ_D can be measured by:

$$P = \emptyset \frac{\Delta\rho}{\rho} \frac{Z_S Z_E}{Z_S + Z_E} \mu_D E \quad (6)$$

Where P is the pressure, E is the electric field, $\emptyset$ is particle volume fraction in the suspension, ρ is the solvent density and $\Delta\rho$ is the difference between particle density and solvent density. Z_s is the acoustic impedance of the suspension, and Z_E is the acoustic impedance of the electrode.

Under different frequency, the dynamic mobility will exhibit different value:

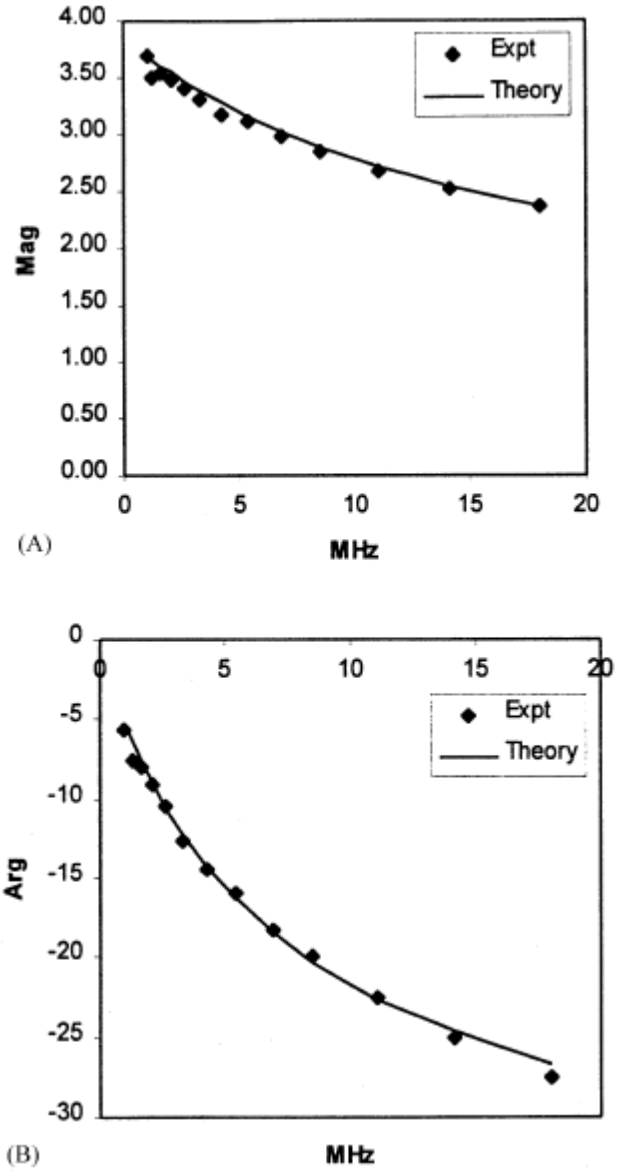

Figure 11 Dynamic mobility as a function of frequency. (A) The magnitude of mobility (B) The phase angle at which the sonic wave delay the electric wave.

Reprinted from R.W. O'Brien, A. Jones, W.N. Rowlands, A new formula for the dynamic mobility in a concentrated colloid, Colloids and Surfaces A: Physicochemical and Engineering Aspects, 218 (2003) 89-101, with permission of Elsevier.

Then using the fitting software in reference [20], the size distribution function will be tried out until the fitting for both the magnitude and the phase angle of dynamic mobility have minimum error. The advantage of sonic wave method includes: 1. The measurement can be performed *in-situ;* 2. Compare to DLS, dilution of the sample is not needed; 3. Works well with opaque sample. However, for a large quantity of biology sample, high frequency oscillation cannot be tolerated, thus this method only with non-organic samples and very limited organic ones.

In sum, although various size detection methods are available, an alternative way to reliably detect the size of the liposomes without damaging the sample is still in need. In next chapter, the resistive pulse method will be demonstrated with liposome sample with good precision and high accessibility, which proves promising in liposome size detection.

CHAPTER 4 EFFECT OF PH STRENGTH ON THE SIZE OF LIPOSOMES

Abstract

A resistive pulse based size measurement method are proposed in this work as an effort to gain more understanding of the property of liposomes, a promising lipid bilayer structure for drug delivery. Liposome samples of 200nm, 100nm, 80nm, and 50nm, fabricated by extrusion technique with polycarbonate filters of corresponding size, are tested employing the resistive pulse method. Good agreement in size distribution are obtained in each size respectively. Further investigation are focused on 100nm liposomes while we tune the inside and outside pH of them to 7, 8 and 9 respectively. Under the influence of pH gradient across the membrane, the sample exhibit various size change. Both osmosis pressure and lipids charge are correlated as potential mechanism for this phenomena, while we proposed that the latter one has the dominating effect on liposome size. The resistive pulse detection of liposome size change will provide invaluable information for studying liposomes as drug delivery vehicles.

Introduction

Vesicles are complex structures composed of lipid bilayer membrane that contain

various materials, such as ions, proteins and peptides [6, 21]. They are formed by budding from the membrane of the internal compartment, or the membrane of the cell. They play an important role as the transporters of materials or information both intracellular and intercellular. For example, in neurons, the synaptic vesicle maintains a reliable transportation and release of the neurotransmitter, thus they are essential to keep the excitation flow within nervous system. Liposomes, on the other hand are self-assembled lipid bilayer colloidal nanoparticles that are prepared using various phosphorous lipids and cholesterols. Since their membrane compositions and size are comparable to the vesicles, liposomes have been used as a model system of vesicles. Typical size of stable liposome is around 50 to 200 nm. However under certain circumstances, low temperature or embedding surface modification for instance, liposomes aggregation could occur [22], which will result in a change in size, charge, and mobility, therefore affect the liposome transport mechanism. It has been reported that exosomes, a type of smaller vesicles, could be a robust bio marker for prostate cancer [23]. Due to their important role in drug delivery, the investigations of liposomes have the potential to improve early stage diagnose of disease and drug delivery system.

Conventionally, chromatography, electron microscopy, and dynamic light scattering technique are used in order to detect and measure the size of liposomes [24-26], which has been reported to be a significant variable affecting the efficiency of drug delivery [11]. It is known that a pH gradient of both natural and synthetic vesicles can affect the size and charge of these vesicles[27]. For example, dynamic light scattering and

transmission electron microscopy have been used to study the effect of pH gradient of vesicles [27-29]. However, there are certain limitations of these techniques [30-32]. Here we describe a method based on the resistive pulse technique to detect the size of liposomes. We investigate the effect of pH gradient across the membrane on the size and charge of liposomes.

Experimental

Preparation of liposomes

Liposomes used in our experiments are prepared by the dehydration-rehydration vesicle method [33]. To entrap KCl solution inside our liposome samples, the initial dehydration solvent used is chloroform and the rehydration solvent used is KCl solution. For 200 nm liposomes we used 0.1 M KCl solution, and the rest of our samples we used 0.5 M KCl solution. The lipids used are 52.5% 1-palmitoyl-2-oleoyl-sn-glycero-3-phosphocholine (POPC), 21% 1-Palmitoyl-2-oleoyl-sn-glycero-3-phosphoethanolamine (POPE), 13% 1-palmitoyl-2-oleoyl-sn-glycero-3-phospho-(1'-myo-inositol)(ammonium salt) (POPI), 3.5% 1-palmitoyl-2-oleoyl-sn-glycero-3-phospho-(1'-rac-glycerol) (POPG), and 10% cholesterol. After rehydration, multi-lamellar liposomes are formed, which have a diameter of a few hundred nanometers.[19, 34] Then these liposomes went through the extrusion procedure to form single lamellar liposomes [35]. We used extruder purchased from Avanti Polar Lipids Inc. with four different size filters (200nm, 100nm, 80nm and 50nm), to obtain the desired liposome size for our investigation. In our later

pH effect measurements, a similar procedure was used with a slightly different lipid composition. The composition of the lipids used in the pH investigation is changed to 50% POPC and 50% POPG in order to produce liposomes with less rigidity, to allow easier access to the liposome size change. During the rehydration of the liposomes, the solvent used for the rehydration is 0.5 M KCl solution with NaH_2PO_4 and Na_2HPO_4 buffer at pH = 6 (4.92 mM of NaH_2PO_4 and 35.08 mM of Na_2HPO_4), or pH = 7 (24.4 mM of NaH_2PO_4 and 15.6 mM of Na_2HPO_4), or pH = 8 (37.88 mM of NaH_2PO_4 and 2.12 mM of Na_2HPO_4) respectively. After rehydration, again multi-lamella liposomes were formed. The solutions went through the extrusion process as described above to form single lamella liposomes. Finally the solution of single lamella liposomes undergoes a gel filtration process using 0.5 M KCl solution with phosphate buffer of the desired pH value (pH = 6, 7, 8 respectively, as described above), such that the pH value of the solution can be changed to the targeted value while keeping the pH value of the liquid entrapped inside the liposomes unchanged. The total lipids concentration we used in this experiment is 0.5mM, for a single 100 nm liposome, we estimate the number of lipids per liposome to be around 80,000, thus the liposome number density is around 3×10^{15} per liter.

Resistive Pulse Method

A Coulter counter is an instrument with the ability to count and to size particles suspended in an ionic solution. A typical Coulter counter is often formed by one or more

micro/nano channels that connect two isolated volumes filled with electrolyte solutions [36]. As fluid containing particles or cells passes through the channel, a brief change in the electrical resistance of the channel occurs. This sudden change in resistance of the channel will result in a current pulse[37]. By monitoring this signal, information such as particle size distribution, mobility, surface charge, and concentration of the particles can be obtained since the magnitude and duration of the current change depends on the charge and the size of the particles [38]. Due to the simple construction of these devices and the reliable sensing method, Coulter devices have found application in a broad range of particle analyzers. In modern hospital, it is widely used as a quick and accurate analytical instrument for blood cell counts [36].

Our resistive pulse technique is based on pulled glass pipettes. The details of our resistive pulse apparatus has been described in a recent publication [39]. Briefly we describe the methodology below: we assume that the normalized current change is proportional to the normalized resistance change [37]. Deblois and Bean [40] proposed an expression for the resistance change due to a particle located inside a micro-channel:

$$\Delta R = \frac{4\rho d^3}{\pi D^4} F \qquad (7)$$

where ΔR is the change of the resistance due to partial blockade of ionic current channel, ρ is the resistivity of the solution, d is the diameter of the particle, D is the

diameter of the channel, and *F* is a correction factor which is a function of d/D .Under these conditions, the size of the particle can be expressed [39]:

$$d = \sqrt[3]{\frac{(\Delta I)V\pi D^4}{4\rho I^2 F}} \quad (8)$$

Experimental set-up

After extrusion, we put about 2 - 5 µl of liposome solution onto a shallow well of a glass substrate, which is located on a microscope stage as shown in Figure 12. Both the micropipette (with measuring electrode) and the reference electrode are fixed on separate micro-manipulator and can be controlled independently. We then carefully bring the micropipette and the reference electrode in and immerse both tips in the liposome droplet. The concentration of the liposomes in the solution is typically 0.5 mM and one typical measurement takes about 2-5 µl of the liposome solution, therefore this method is ideal for minute amount of sample.

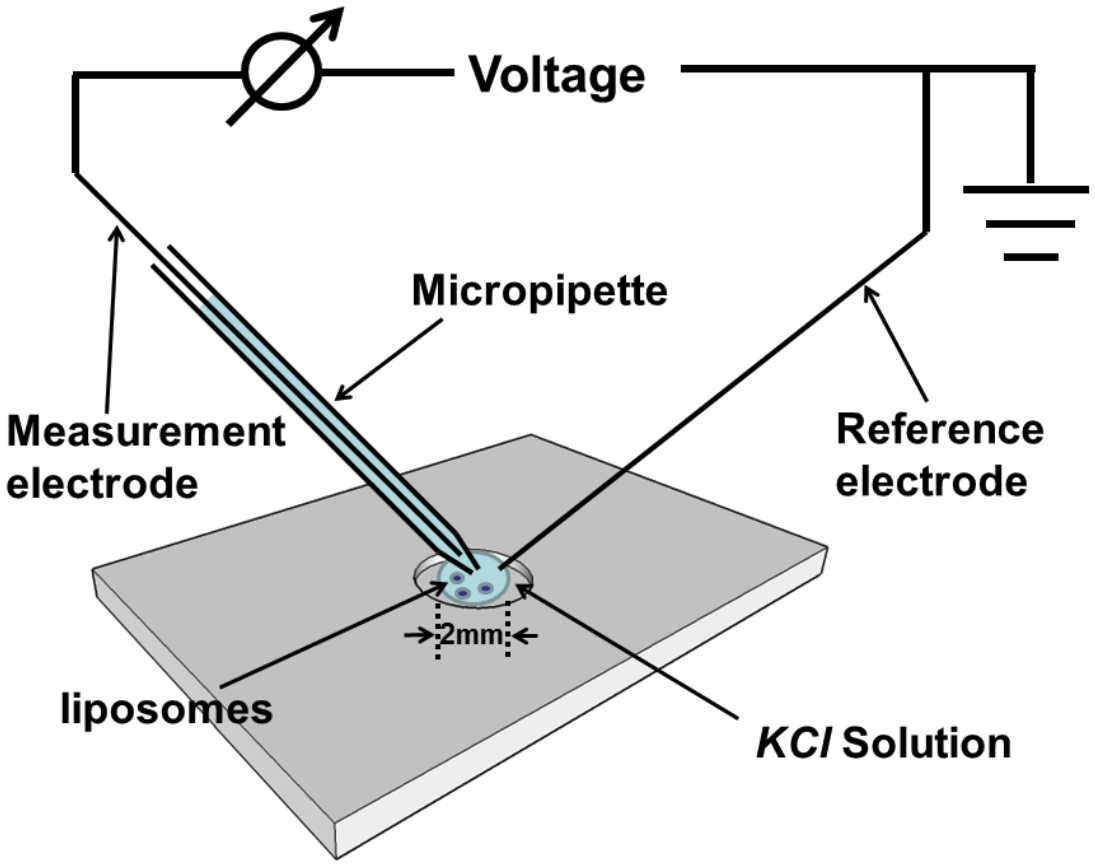

Figure 12 Schematic diagram of the experimental set-up. A glass slide is position on a stage under a microscope. Both the micropipette and the reference electrode are on separate micro-manipulator.

An Axopatch 200B amplifier in voltage clamp mode serves as both the voltage source and the current meter. The current pulse signals are recorded by AxoScope 10.2 using Axon Instrument Digidata 1440A Series at a sampling rate of 250 kHz and a bandwidth of 2 kHz. The electrodes used are two 0.2 mm diameter Ag/AgCl wires; one inserted into the open end of a micropipette of inner diameter of 0.8mm, while the second electrode served as a counter electrode. The KCl solution inside the micropipette is the

same as the KCl solution containing liposomes.

Results

In Figure 13, we showed the translocation data for four different sizes of liposomes. Each translocation event is displayed in the current vs. time plot as a negatively going current spike. The baseline current is determined by the size of the nanopore, the strength of the ionic solution and the voltage applied to the two electrodes. We noticed that the baseline currents showed some weak decay or slight linear increase as a function of time. These minute variation of the baseline current may be attributed to charging or discharging effect or electrochemical reaction as the surface of the electrodes or glass capillary. Since the magnitudes of these changes are quite small, we believe it will not affect our size measurements. Each translocation event can be quantified into a data point [41], of which the x and y coordinates represent the translocation duration and the current amplitude respectively in the scatter plot shown in inserts of Figure 14.

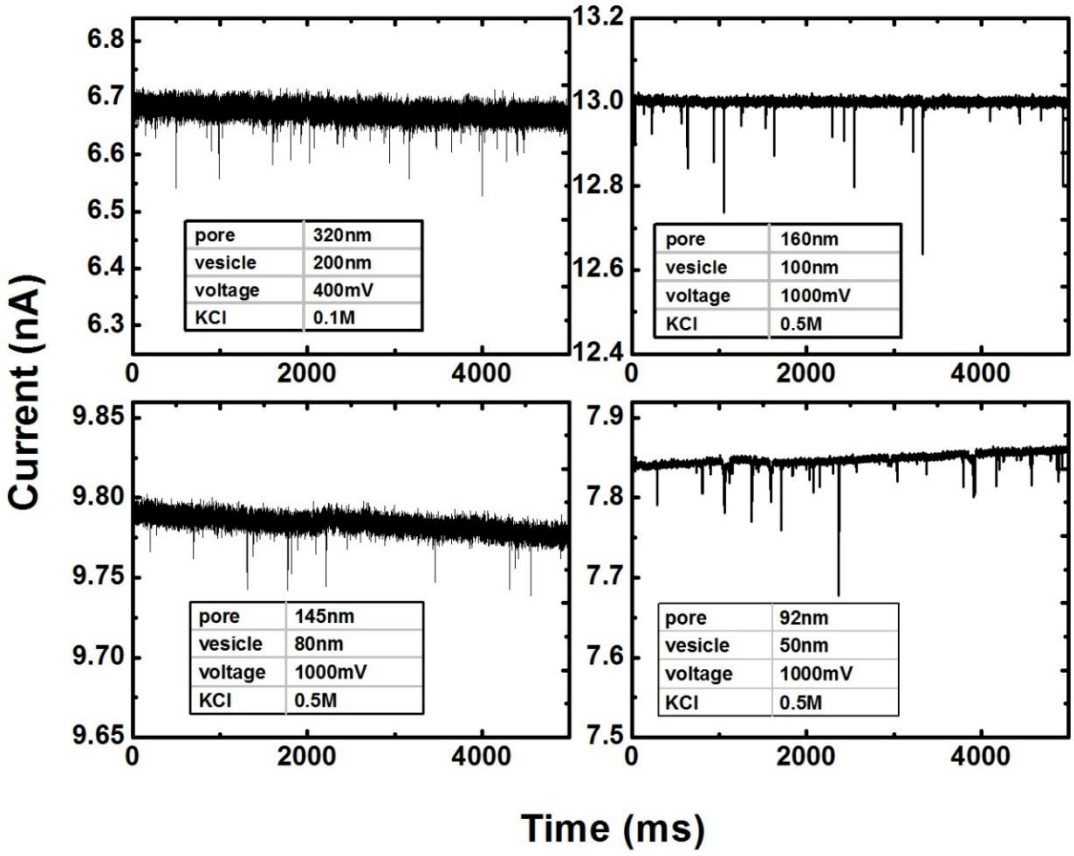

Figure 13 Translocation current as a function of time for four different sizes of liposomes. For each set of measurements, micropipette with a different pore size is used. The measurement conditions are shown on each drawing.

In Figure 14, the measured size distribution of the liposomes produced using the extruder method with different sizes of filters are shown. These filters are purchased from Avanti Company. The diameters of the liposomes are calculated from the translocation data using equation7. From these histograms, the mean values and the standard deviations of each distribution are calculated and are listed in Table 4.

Table 4 Liposome size with different extruders under pH7

Extruder size	200nm	100nm	80nm	50nm
Measured size	205.9 ± 30.1nm	113.7 ± 9.1nm	80.8 ± 7.6nm	55.3 ± 15.4nm

From these results, we can see that the diameters of the liposomes measured using our micropipette based resistive pulse method agreed with the size of the filter used in the extrusion method. We also noticed that the standard deviations of the size distribution for the 80 nm and 100 nm filters are much smaller than that of the 50 nm or 200 nm filters. This is quite reasonable, it is well-known that extrusion with a filter size of 200 nm and higher produced a highly poly-dispersive liposomes [34], while liposomes with a diameter of 50 nm and lower [42] are unstable due to the high degree of curvature near the interface. Hence we choose the optimal size of 100nm for the rest of our experiments to investigate the effect of pH gradient on the size of liposomes.

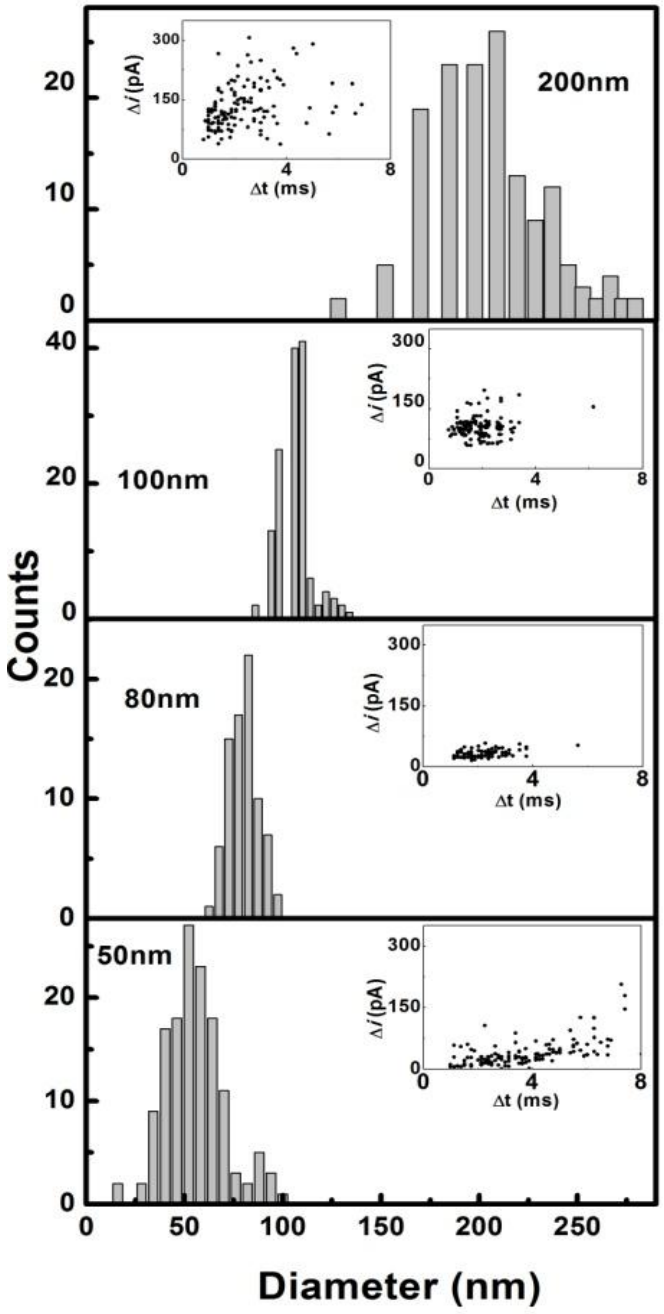

Figure 14 Size distribution of liposomes prepared by the dehydration-rehydration method. (a) D = 200 nm, (b) D = 100 nm, (c) D = 80 nm, (d) D=50 nm. The corresponding scatter plots are also shown.

The correlation between pH and the properties of liposomes has been investigated by previous publications using various technique [43], for example, Hafez *et al* performed visual inspection of liposome at different pH environment using Freeze-fracture electron microscopy, to study the fusion and formation of lipids membrane.[44] Guo *et al* have observed POD/POPE/DOPE liposome leakage of ANTS/DPS as a function of pH. The lag time for leaking increases as pH goes up.[45] Bitbol *et al* detected the formation change, to help understanding the stability, under pH gradient by adding NaOH to the solution outside the liposomes. Fluorescence microscopy and phase contrast microscopy pictures are taken as a function of time. [46] Zhang et al fabricated perylene bisimide chromophores liposomes that emit fluorescence under different pH environment [47], among many other important properties of liposomes. Our focus has been on the pH effect on the size of liposomes. Certain limitations exits while DLS and Cryo TEM have been used mainly as a standard process for size measurement [18, 19, 48], thus, other efforts like fluorescence [49] or supersonic wave [20] are developed. However, fluorescence method may intervene other commonly used fluorescence-based measurement like leakage test, and supersonic wave may potentially damage the less stable liposome sample. As a result, both methods are limited in application. Our resistive pulse method serves as an alternative technique, as it delivers single particle resolution, low sample interference. Thus, the data presented here, may be helpful in shedding some light on the effect of pH on the size change of liposomes.

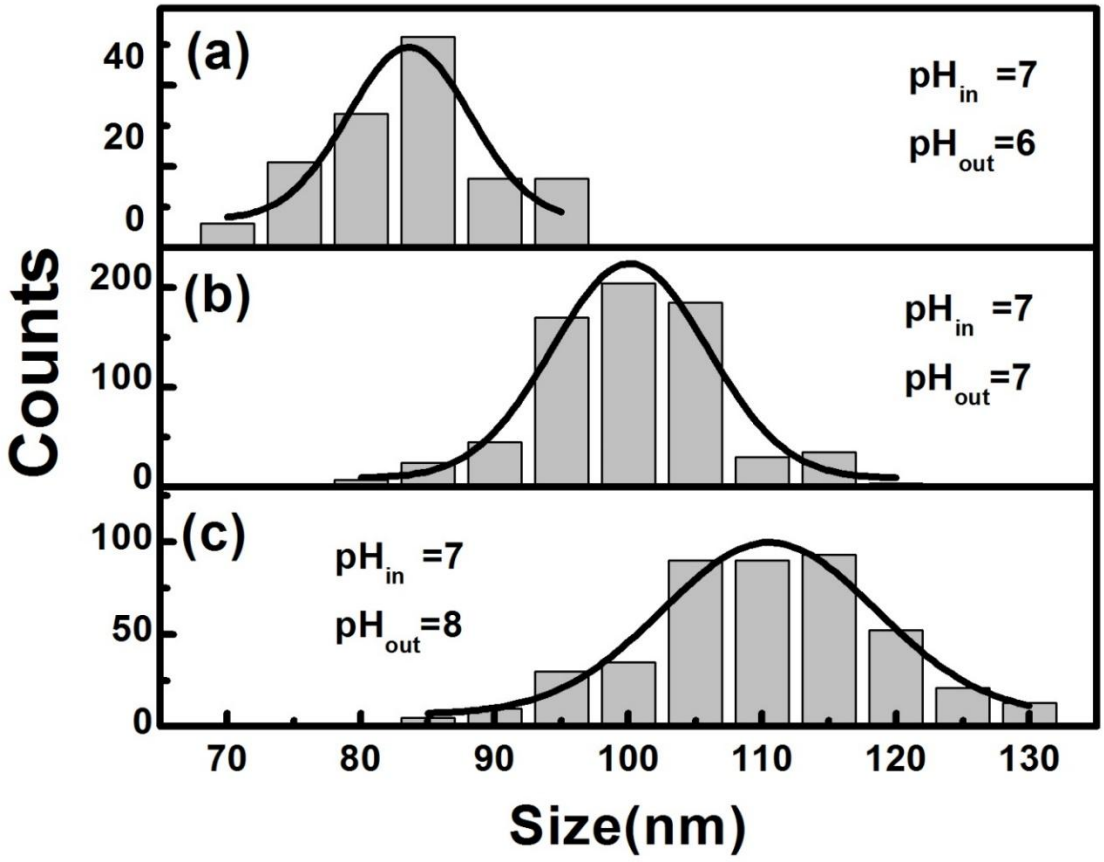

Figure 15 Size distribution of liposomes with (a) internal pH value of 7 and external pH value of 6, (b) internal pH value of 7 and external pH value of 7, (c) internal pH value of 7 and external pH value of 8.

In Figure 15, we show the size distribution of liposomes which were initially rehydrated in 0.5M KCl solution with pH value of 7. After extrusion, the outside solution's pH value is changed to pH = 6 or 8 using gel filtration. From Figure 15, we noticed a size change as we change the outside solution's pH value. In Figure 15 (b), when pH_{in} = 7 and pHh_{out} = 7, the radius of liposomes is determined to be 100 nm, which agrees well with

the extruder size, i.e. 100nm. For the same liposomes, when we increase the pH_{out} to 8, the size of the liposomes increases to about 110 nm. As the pH_{out} decreases to 6, the size decreases to about 85 nm. As we can see there are two different phenomena at play here, i.e. (a) The size of the extruded liposomes seems to depend on the pH value of the re-hydrated solution even when there is no pH gradient across the liposome membrane, (b) The size of the extruded liposomes seem to depend on the pH gradient across the liposome membrane, as we can see in Figure 15.

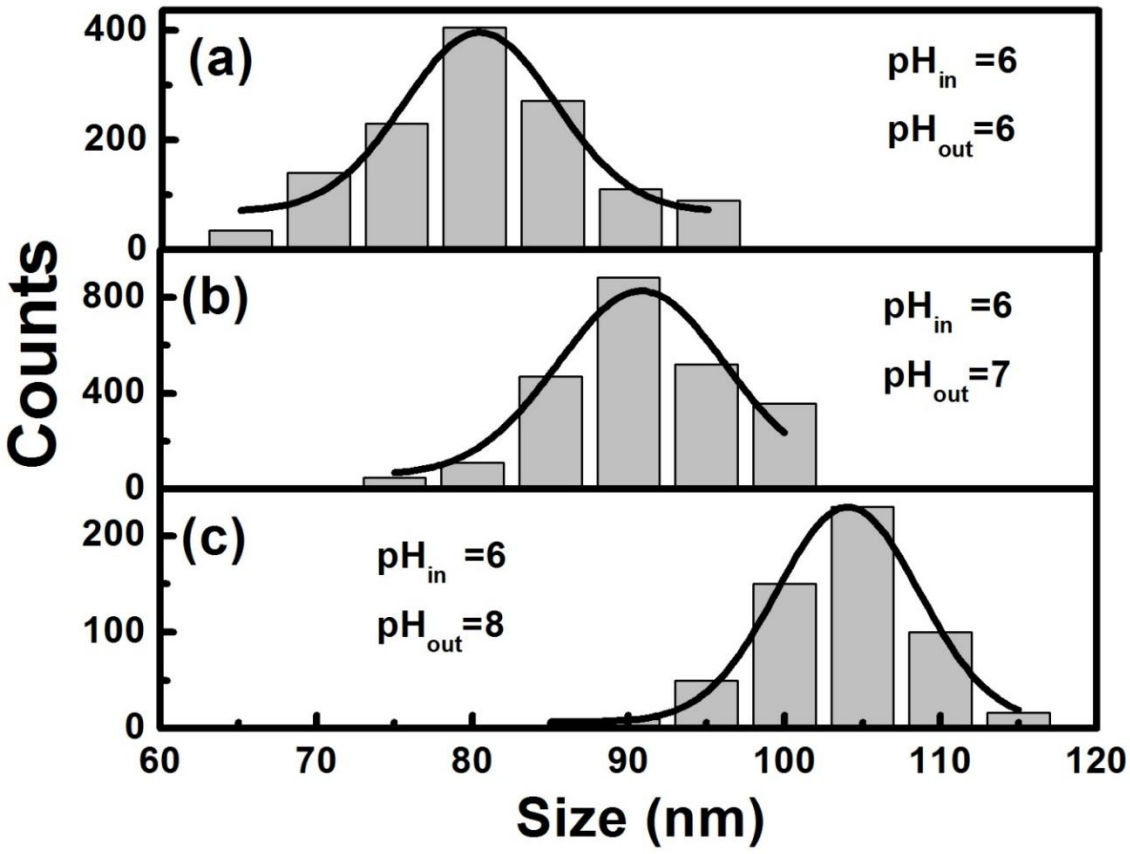

Figure 16 Size distribution of liposomes with (a) internal pH value of 6 and external pH value of 6, (b) internal pH value of 6 and external pH value of 7, (c) internal pH value of 6 and external pH value of 8.

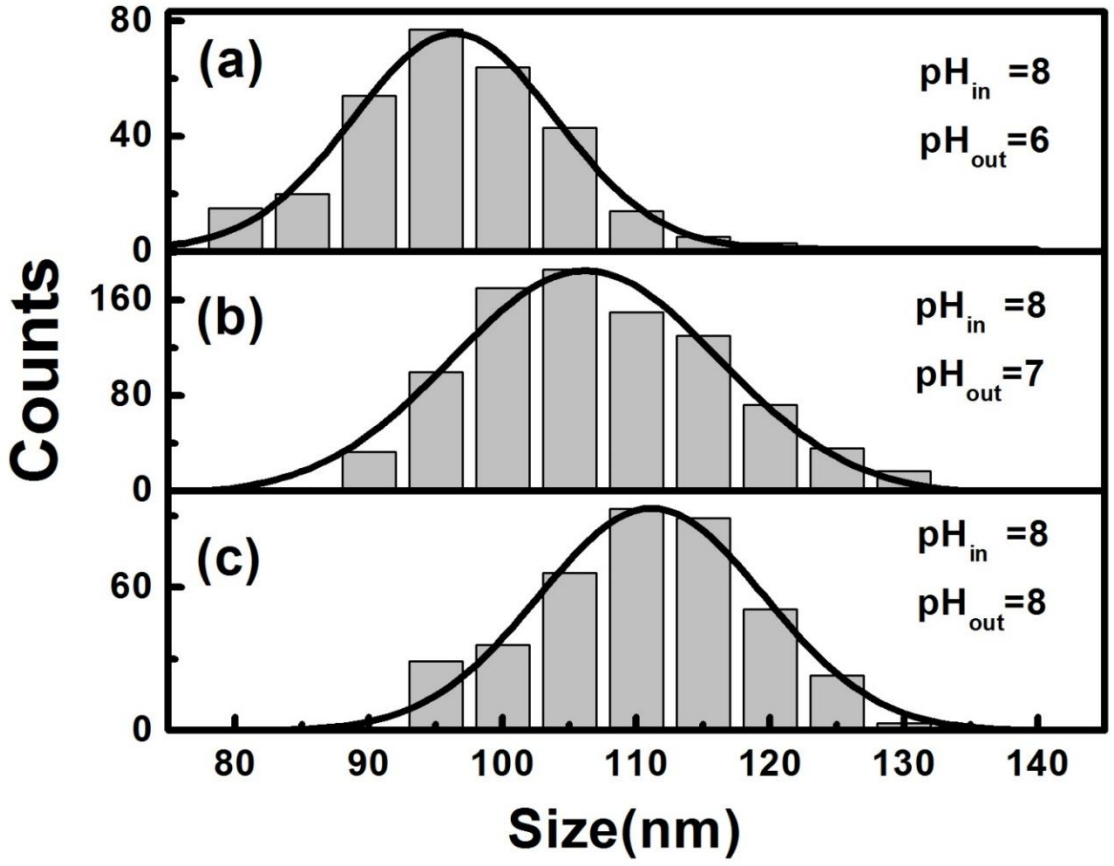

Figure 17 Size distribution of liposomes with (a) internal pH value of 8 and external pH value of 6, (b) internal pH value of 8 and external pH value of 7, (c) internal pH value of 8 and external pH value of 8.

To verify the above observation is a general phenomenon, we repeat the above experiment, using starting 0.5M KCl rehydration solutions with pH_{in} = 6 and pH_{in} = 8. The results are plotted in Figure 5 and Figure 6. In Figure 5, for pH_{in} = 6 and pH_{out} = 6 the size of the extruded liposomes exhibit an average diameter of about 82nm, even though the extruder employed are of 100nm. As we increase the pH_{out} to 7 and 8, the

size of the liposomes changes to 90 nm and 105nm respectively. Similarly when the liposomes are prepared with pH_{in} = 8 and pH_{out} = 8 with zero pH gradient across the membrane, the size of the liposomes increases to 104 nm. As we decrease the pH_{out} of the outside solution to 6 or 7, the size of the extruded liposomes decreases to 80 nm or 92 nm respectively as shown in Figure 6 (a) and Figure 6 (b). The complete information regarding the pH dependence of size are summarized in table 2.

Table 5 Liposome size under various pH conditions

pH outside / pH inside	6	7	8
6	80.5 ± 6.5nm	90.8 ± 5.8nm	103.6 ± 5.2nm
7	83.5 ± 6.4nm	100.0 ± 6.9nm	109.9 ± 8.7nm
8	96.5 ± 5.8nm	107.1 ± 7.5nm	110.7 ± 7.2nm

The rigidity of the liposomes are dependent on the Debye layer length[50], which is constant due to the domination of ion concentration by 0.5M KCl, comparing to pH gradient thus proton concentration, throughout all of our experimental environment.

This phenomenon suggests that other than the osmotic pressure, electric charge that lipids carry might also play a role in the size change of liposomes, regarding the fact

that the rigidity remains constant thus cannot be the reason of size change. As previously reported [51, 52], charge is of great importance in determining the shape and formation of the vesicles. With our method, we are able to quantify the change in size as the pH condition varies. Increasing the pH will make the lipids which form vesicles carry more negative charge, therefore the lipids will have stronger repulse to each other, resulting in larger vesicle size.

Under the circumstances of an existing pH gradient, the water molecule, being much more permeable to lipid bilayer membranes than ions[53], will move from low proton concentration environment (and therefore high pH) to high proton concentration environment(low pH), resulting in the swelling or shrinking of the vesicle size.

To estimate the effect of pH on the charge, we use the data from the Avanti website (http://avantilipids.com/index.php?option=com_content&view=article&id=1598&Itemid=379) and the zeta potential-pH relationship found on reference[52].Initially, when pH=7, the charge is 1 electron charge, and we estimate in 100nm vesicles there are about 85000 lipids per vesicle, so the total charge is 42500 electron charge, due to the composition only half of the lipids carry charges.

Consider any great circle of a liposome. The sum of neighboring lipids' repelling forces due to coulomb interaction along that great circle will be the tension force. We can compare that to the known value of the surface tension of lipids. Note that the coulomb

interaction will have different intensity since the charge of the lipids changes at different pH.

From the total number of the charged lipids and the diameter of the liposomes we can get the number density of lipids on the liposome surface, and the estimation of the neighboring distance. Summing all the coulomb repelling forces, we have $F_{pH=7} = 9.79 \times 10^{-8}N$, $F_{pH=6} = 5.37 \times 10^{-8}N$, $F_{pH=8} = 1.44 \times 10^{-7}N$. Comparing from the surface tension data we have from reference [54], we have $T_{pH=7} = 8.48 \times 10^{-8}N$, $T_{pH=6} = 7.63 \times 10^{-8}N$, $T_{pH=8} = 9.33 \times 10^{-8}N$. The coulomb force and the surface tension are in the similar order of magnitude, and they exhibt the same trend when the pH-caused size change occurred.

On the other hand, we can estimate the effect of the possible osmosis pressure caused by pH gradient using Morse equation. The estimated force is around 1.5×10^{-14}N, which is significantly smaller than the effect of charge change. This might suggest that pH effect on charge is the dominating reason for the liposome size change we observed.

Conclusion

In summary, we have been able to demonstrate reliable and accessible method of measuring various sizes of liposome and successfully identify the size change under a pH gradient environment. We propose that this phenomenon is caused by the variant charge of which lipids that forms the liposomes carry under different pH. Although

further experiments are needed to confirm this explanation, we hope the information that liposome size change under pH gradient will provide some helpful information for finely tune the efficiency for liposome based drug delivery research.

Acknowledgment

This material is based upon work supported by the National Science Foundation under Grant ECCS 0901361. Any opinions, findings, and conclusions or recommendations expressed in this material are those of the authors and do not necessarily reflect the views of the National Science Foundation.

CHAPTER 5 RESISTIVE PULSE STUDY OF THE STABILITY OF SUV (SMALL UNILAMELLAR VESICLES)

Motivation

Due to the lipid bilayer structure and convenient fabrication, liposomes has become of great interest among the drug delivery research community. An ideal candidate as anti-cancer drug delivery vehicle, liposomes, along with their physical and chemical properties has been essential to effective drug delivery.

Among the many properties of the liposomes, size has been one dominate variable in determining the circulation time, ability to penetrate tight tissue, and drug loading efficiency. In particular, the SUV (small unilamellar vesicles) has drawn the attention of the researchers since some of the tumor tissue are condensed, the spacing between which are below 100nm. Therefore, as drug delivery vehicle, only liposomes with lower than 100nm diameter can pass through, which makes SUV liposomes (diameter ranges from 100 to 20nm) a promising solution in this situation.

However, the problem of SUV liposomes exists: the small size of liposomes brings high curvature to the lipid bilayer structure which makes the tension among lipids high and thus the liposomes are less stable. [42, 55, 56] Fusion among the smaller liposomes happens, results in not only possible leaking of the loaded drugs, but also significantly alter the circulation time. The bigger liposome will also fail to pass through the more condensed tissue, leading to low efficiency or even failure to the delivery.[57, 58]

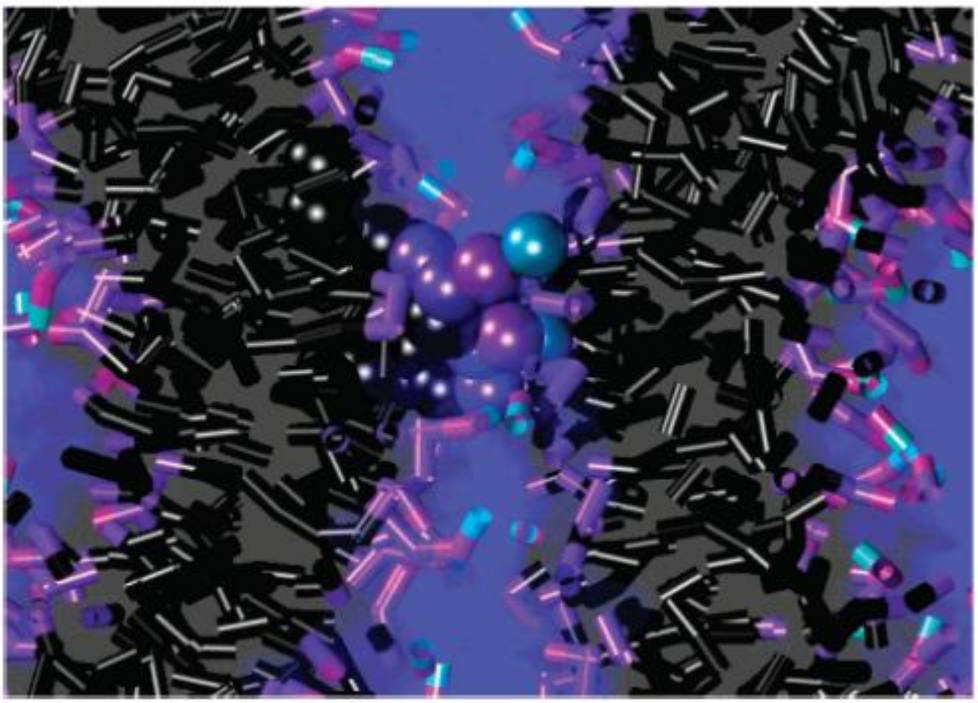

Figure 18 Simulation of the beginning of fusion between two liposomes. Reprinted with permission from S.J. Marrink, A.E. Mark, The Mechanism of Vesicle Fusion as Revealed by Molecular Dynamics Simulations, Journal of the American Chemical Society, 125 (2003) 11144-11145. Copyright (2003) American Chemical Society

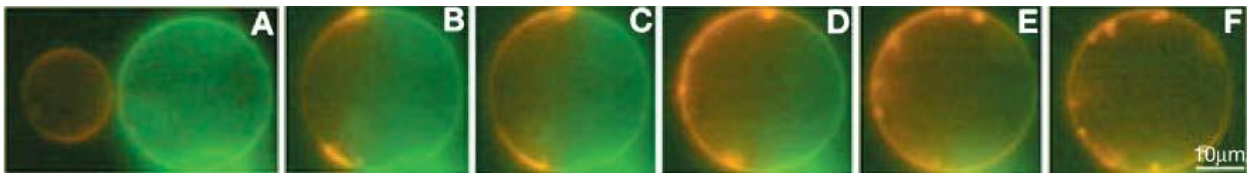

Figure 19 Fluorescence image of fusion vesicles, Reprinted from G. Lei, R.C. MacDonald, Lipid Bilayer Vesicle Fusion: Intermediates Captured by High-Speed Microfluorescence Spectroscopy, Biophysical Journal, 85 (2003) 1585-1599, with permission from Elsevier

To overcome this difficulty, various efforts, including nanoparticle coating(as shown in Figure 20) [59-61], inject environment solution with cholate salt [62], and polyvinyl

alcohol coating[63] have been made to enhance the stability of liposomes by preventing or delaying fusion. The methods all work to a certain extent, however, many of the drugs which require liposomes as delivery vehicles are toxic to normal cells, more details about the stability of liposomes, especially SUV liposomes, need to be studied. In this work, we are aiming to get more knowledge about the SUV fusion process using resistive pulse method that was developed in-house, thus provide more useful information to help improving the stability of SUVs.

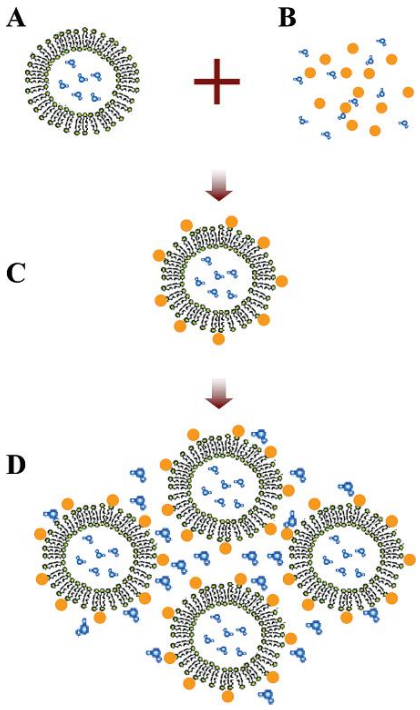

Figure 20 nanoparticle stabilizing liposomes. (A) liposomes (B) Polystyrene nanoparticles (C) Mix liposomes and nanoparticles with a molar ratio of 1:100 and undergo 10min of sonication (D) gently blow nitrogen gas to improve the distribution of the suspension. Reprinted with permission from L. Zhang, S. Granick, How to Stabilize Phospholipid Liposomes (Using Nanoparticles), Nano Letters, 6 (2006) 694-698. Copyright 2006 American Chemical Society

Experiment

The SUV we used in this work have a composition of 50% 1-palmitoyl-2-oleoyl-sn-glycero-3-phosphocholine (POPC), and 50% 1-palmitoyl-2-oleoyl-sn-glycero-3-phospho-(1'-rac-glycerol) (POPG). The classical dehydration-rehydration method is employed to prepare the liposomes, the detail of this method can be found in our previous publication [39]. The liposomes are extruded with a 50nm Avanti Inc. polycarbonate extruder for 20 times in pH=7, 0.1mM KCl solution environment. The total volume of solution after the extrusion is about $30\mu l$, with a lipid concentration of 0.5mM.

Immediately after the preparation, the SUV samples are measured by resistive-pulse method as a function of time. The details of resistive pulse method can also be found in our previous work[39]. The size distribution of the SUV are obtained at 30min, 60min, 90min, 120min, 240min, 480min, 720min, and 960min. The sample are then tested at 1200min using dynamic light scattering system from Malvern (Zetasizer Nano Z) to crosscheck the results with resistive pulsing method.

Results

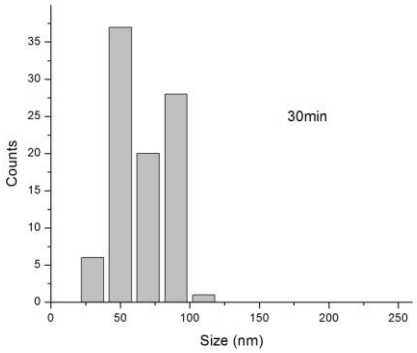
30min
Counts
Size (nm)

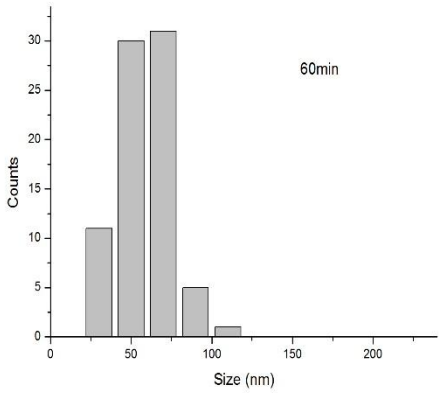
60min
Counts
Size (nm)

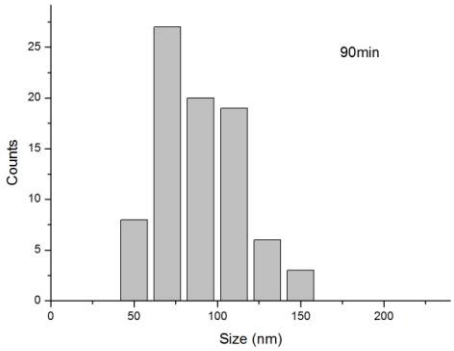
90min
Counts
Size (nm)

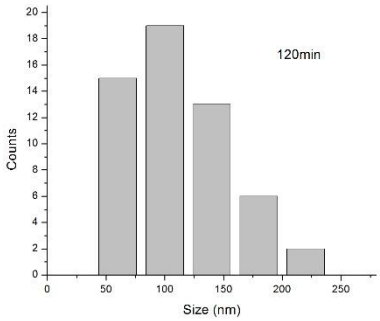
120min
Counts
Size (nm)

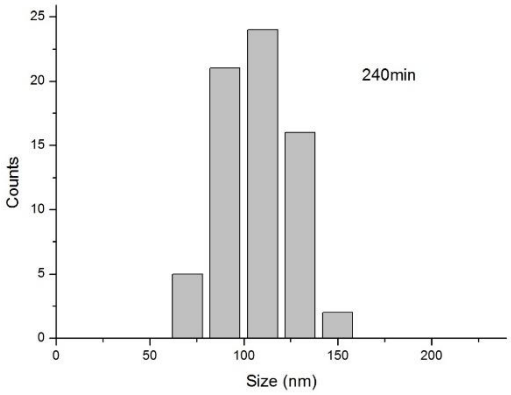
240min
Counts
Size (nm)

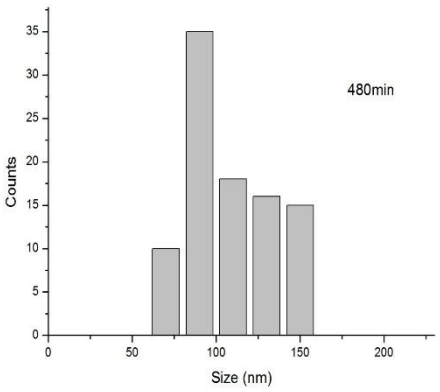
480min
Counts
Size (nm)

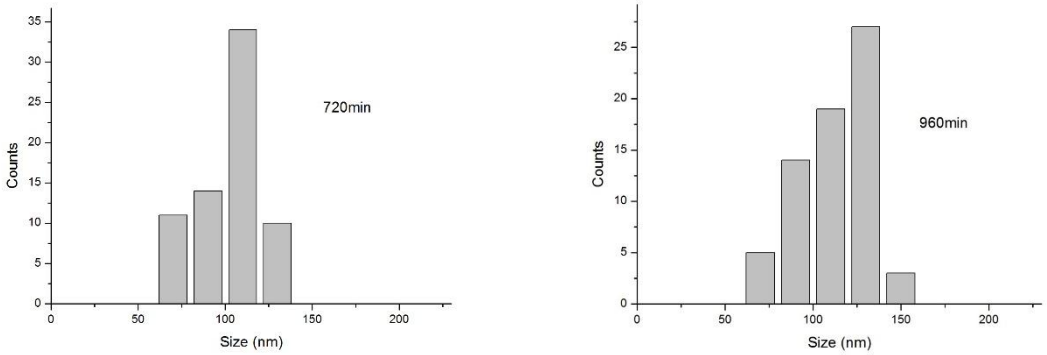

Figure 21 Size distribution measured by resistive pulse method as a function of time (30min, 60min, 90min, 120, 240min, 480min, 720min, 960min)

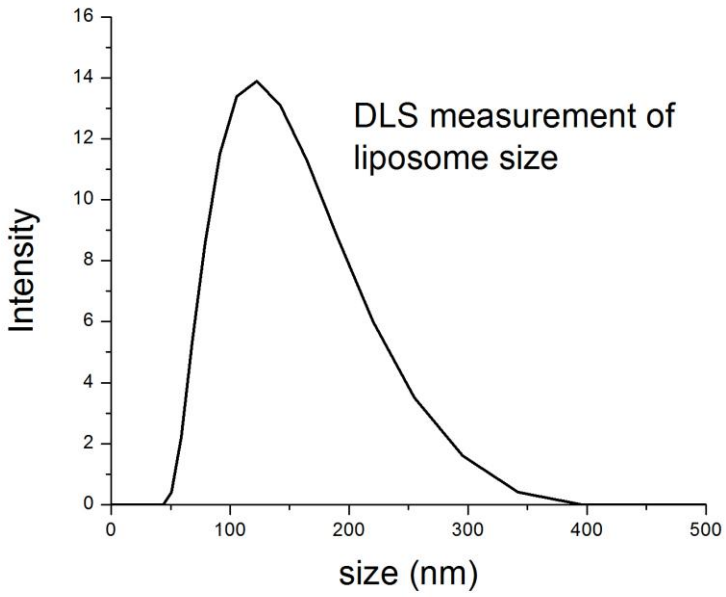

Figure 22 Dynamic light scattering size measurement at 1200min after the sample was prepared

As illustrated in Figure 21 and Figure 22, the size distribution data obtained via resistive pulse method and DLS clearly demonstrate the average size shifting to larger size, potentially due to liposomes fusion. To get a more intuitive view, we plot the average size vs. time, as shown in Figure 23.

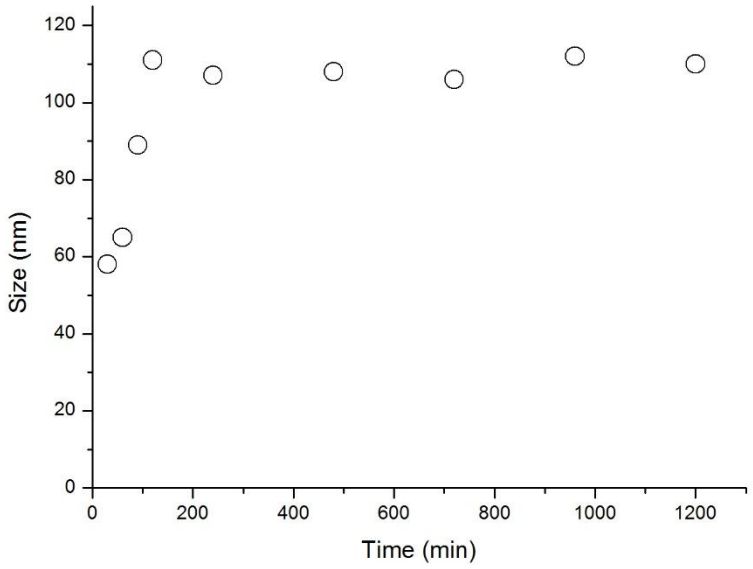

Figure 23 Average size as a function of time. All the data points are based on resistive pulse method except the one at right hand side (at 1200min), which is based on the DLS data from Figure 22

Discussion

The plot of size vs. time indicated that in the first hour after the 50nm SUV are freshly prepared, the size almost remained close as their intended extruded size, however during the second hour the size of the SUV went through drastic increase, until at two hours the liposomes reaches around 110nm in diameter, and the size remains at that

value all the way through 20 hours with a less than 5nm fluctuation in average diameters.

There are two possible fusion mechanism that could be involved here. The first possible scenario is hemifusion. Hemifusion happens when two liposome have contact with each other and the lipid bilayer opened up at the location where the contact is. The opened parts of bilayer connect again but further fusion is not going on. It is believed that with the presence of cholesterol hemifusion will be an intermediate stage[64]. In our case, the hemifusion stage could be a stable, final stage[56], without the existence of cholesterol.

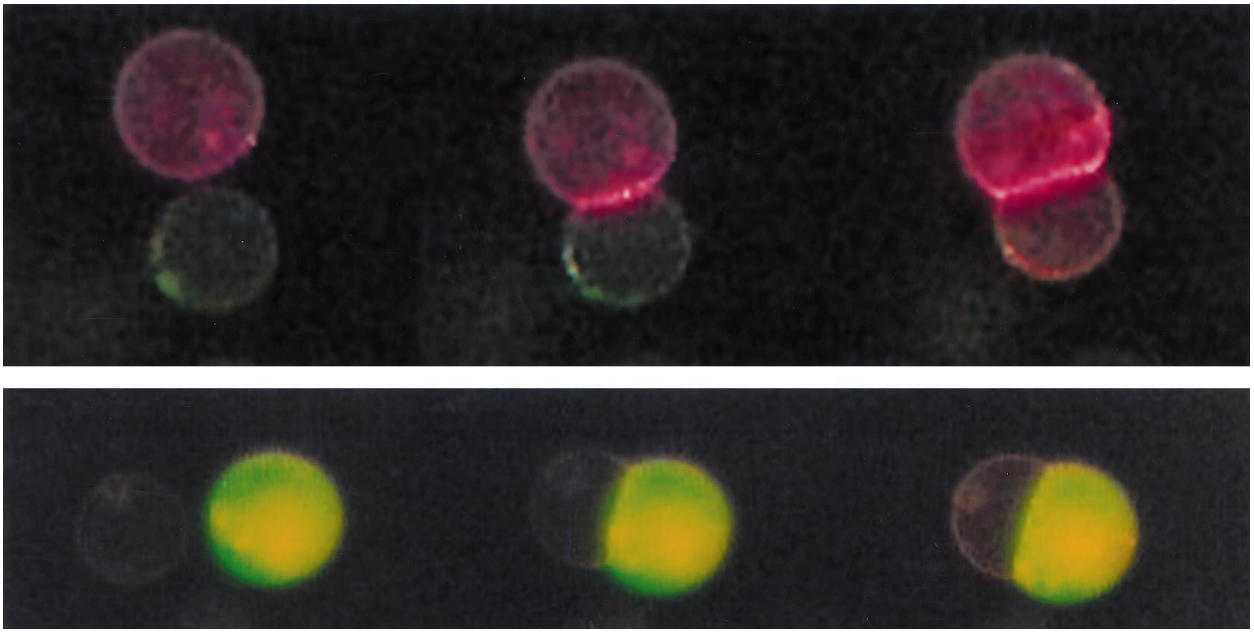

Figure 24 Visualization of hemifusion in different dye. Reprint from R.A. García, S.P. Pantazatos, D.P. Pantazatos, R.C. MacDonald, Cholesterol stabilizes hemifused phospholipid bilayer vesicles, Biochimica et Biophysica Acta (BBA) - Biomembranes, 1511 (2001) 264-270, with permission from Elsevier

This model could explain the stable size we detected. The longitudinal length is twice the original diameter, but in the assumption of resistive pulse method we simplify the problem by treating all the particle as spherical. The similar assumption is also applied in DLS method.

Another possibility is full fusion. As its name indicates, full fusion is the scenario when two liposomes completely fused together. In this case, two 50nm liposomes fuse together, to become a larger, perfect spherical shape liposome. The pH and salt concentration remain the same as fusion goes on, so the charge on the lipids should be the same, therefore the arrangement, or the average distance from one lipid to its neighboring lipids, should remain the same. The new liposome's surface area should be equal to the sum of two parent liposomes. This will result in the diameter equaling to $\sqrt{2}$ times of the diameter of its parent liposome. This could be the reason we detect liposome of diameter between 50nm to 100nm at the second hour. After the fist full fusion, the curvature of the liposome are still high, therefore the second full fusion will bring the size to 100nm.

The duration of fusion process, for both hemifusion and full fusion, is on the level of milliseconds[56]. However the fusion need to be initialized by contact. In our experiment, all the liposome carries negative charge[39], the repulsive interaction makes it difficult for contact to occur. The high curvature of 50nm liposome break a small part of the bilayer after Brownian motion for a while, make it possible for contact to occur and also serves as the reason for lipids to open a small portion for fusion to begin. It is not clear

what is the exact driving force for fusion, while entropy is considered as a good candidate[64].

APPENDIX: PUBLICATION LIST

Journals

- “Characterization of liposomes and silica nanoparticles using resistive pulse method”, Colloids and Surfaces A: Physicochemical and Engineering Aspects, 2014
- “Effect of ph strength on the size of liposomes”, to be submitted
- “Resistive pulse study of the stability of suv”, to be submitted
- “Eu-doped ZnO nanowire arrays grown by electrodeposition”, Applied Surface Science, 2013
- “Cathodoluminescence studies of electron irradiation effects in n-type ZnO”, Journal of Physics: Condensed Matter, 2011
- Minority carrier transport in p-ZnO nanowires”, Journal of Applied Physics, 2011
- “Electrically pumped waveguide lasing from ZnO nanowires”, NATURE nanotechnology, 2011
- “Optical and electron beam studies of carrier transport in quasibulk GaN”, Applied Physics Letters, 2009

Conferences

- “Study of vesicle size distribution dependence on pH value based on nanopore resistive pulse method”, APS march meeting, Baltimore, 2013

- “Vesicles sensing using resistive-pulse method”, APS march meeting, Baltimore, 2013
- “Copper doped zinc oxide micro-and nanostructures for room-temperature sensorial applications”, CAS international semiconductor conference, Bucharest, Romania, 2013
- “Optical and sensory properties of ZnO nanofibrous layers grown by magnetron sputtering”, CAS international semiconductor conference, Bucharest, Romania, 2012
- “Rapid hydrothermal synthesis of zinc oxide nanorods on single crystal sapphire substrate”, CAS international semiconductor conference, Bucharest, Romania, 2011
- “Cathodoluminescence study of silver and gold lamellar gratings”, SPIE Proceedings, 2011

Patent

- Capillary ionic transistor: Fabrication and Applications, United States US#61/944,753. Filed 02/26/14

LIST OF REFERENCE

[1] J.C.H.L. Parthiban Chinnagounder Periyasamy, Pieter J. Dijkstra, Marcel Karperien, and Janine N. Post, Nanomaterials for the Local and Targeted Delivery of Osteoarthritis Drugs, Journal of Nanomaterials, 2012 (2012) 13.

[2] F. Yang, C. Jin, Y. Jiang, J. Li, Y. Di, Q. Ni, D. Fu, Liposome based delivery systems in pancreatic cancer treatment: From bench to bedside, Cancer Treatment Reviews, 37 (2011) 633-642.

[3] F. Yan, J. Texter, Capturing nanoscopic length scales and structures by polymerization in microemulsions, Soft Matter, 2 (2006) 109-118.

[4] A.E. Walsby, Gas vesicles, Microbiological Reviews, 58 (1994) 94-144.

[5] S.O. Rizzoli, W.J. Betz, Synaptic vesicle pools, Nat Rev Neurosci, 6 (2005) 57-69.

[6] K. Ikeda, J.M. Bekkers, Counting the number of releasable synaptic vesicles in a presynaptic terminal, Proceedings of the National Academy of Sciences, 106 (2009) 2945-2950.

[7] T.C. Südhof, THE SYNAPTIC VESICLE CYCLE, Annual Review of Neuroscience, 27 (2004) 509-547.

[8] S.Y. Wang, D.B. Tikhonov, J. Mitchell, B.S. Zhorov, G.K. Wang, Irreversible block of cardiac mutant Na+ channels by batrachotoxin, Channels (Austin, Tex.), 1 (2007) 179-188.

[9] Y.A. Ushkaryov, K.E. Volynski, A.C. Ashton, The multiple actions of black widow spider toxins and their selective use in neurosecretion studies, Toxicon, 43 (2004) 527-542.

[10] H.-I. Chang, M.-K. Yeh, Clinical development of liposome-based drugs: formulation, characterization, and therapeutic efficacy, International Journal of Nanomedicine, 7 (2012) 49-60.

[11] A. Nagayasu, K. Uchiyama, H. Kiwada, The size of liposomes: a factor which affects their targeting efficiency to tumors and therapeutic activity of liposomal antitumor drugs, Adv Drug Deliv Rev, 40 (1999) 75-87.

[12] D. Papahadjopoulos, T.M. Allen, A. Gabizon, E. Mayhew, K. Matthay, S.K. Huang, K.D. Lee, M.C. Woodle, D.D. Lasic, C. Redemann, Sterically stabilized liposomes: improvements in pharmacokinetics and antitumor therapeutic efficacy, Proceedings of the National Academy of Sciences of the United States of America, 88 (1991) 11460-11464.

[13] A. Gilert, M. Machluf, Nano to micro delivery systems: targeting angiogenesis in brain tumors, Journal of Angiogenesis Research, 2 (2010) 20.

[14] S. Li, D. Xing, J. Li, Dynamic Light Scattering Application to Study Protein Interactions in Electrolyte Solutions, Journal of Biological Physics, 30 (2004) 313-324.

[15] D.G. Dalgleish, F.R. Hallett, Dynamic light scattering: applications to food systems, Food Research International, 28 (1995) 181-193.

[16] T.G. Mason, H. Gang, D.A. Weitz, Rheology of complex fluids measured by dynamic light scattering, Journal of Molecular Structure, 383 (1996) 81-90.

[17] G.F. White, K.I. Racher, A. Lipski, F.R. Hallett, J.M. Wood, Physical properties of liposomes and proteoliposomes prepared from Escherichia coli polar lipids, Biochimica et Biophysica Acta (BBA) - Biomembranes, 1468 (2000) 175-186.

[18] B. Coldren, R. van Zanten, M.J. Mackel, J.A. Zasadzinski, H.-T. Jung, From Vesicle Size Distributions to Bilayer Elasticity via Cryo-Transmission and Freeze-Fracture Electron Microscopy, Langmuir, 19 (2003) 5632-5639.

[19] A.H. Kunding, M.W. Mortensen, S.M. Christensen, D. Stamou, A Fluorescence-Based Technique to Construct Size Distributions from Single-Object Measurements: Application to the Extrusion of Lipid Vesicles, Biophysical Journal, 95 (2008) 1176-1188.

[20] R.W. O'Brien, A. Jones, W.N. Rowlands, A new formula for the dynamic mobility in a concentrated colloid, Colloids and Surfaces A: Physicochemical and Engineering Aspects, 218 (2003) 89-101.

[21] F. Howard, I. Levin, Lipid Vesicle Aggregation Induced by Cooling, International Journal of Molecular Sciences, 11 (2010) 754-761.

[22] R. Jahn, T. Lang, T.C. Südhof, Membrane Fusion, Cell, 112 (2003) 519-533.

[23] P. Mitchell, J. Welton, J. Staffurth, J. Court, M. Mason, Z. Tabi, A. Clayton, Can urinary exosomes act as treatment response markers in prostate cancer?, Journal of Translational Medicine, 7 (2009) 4.

[24] K. Sakai-Kato, S. Ota, K. Hyodo, H. Ishihara, H. Kikuchi, T. Kawanishi, Size separation and size determination of liposomes, Journal of Separation Science, 34 (2011) 2861-2865.

[25] D.J. Woodbury, E.S. Richardson, A.W. Grigg, R.D. Welling, B.H. Knudson, Reducing liposome size with ultrasound: bimodal size distributions, Journal of liposome research, 16 (2006) 57-80.

[26] S. Hupfeld, A.M. Holsaeter, M. Skar, C.B. Frantzen, M. Brandl, Liposome size analysis by dynamic/static light scattering upon size exclusion-/field flow-fractionation, Journal of nanoscience and nanotechnology, 6 (2006) 3025-3031.

[27] J.C. Selser, Y. Yeh, R.J. Baskin, A light-scattering characterization of membrane vesicles, Biophysical Journal, 16 (1976) 337-356.

[28] W. Li, T.S. Aurora, T.H. Haines, H.Z. Cummins, Elasticity of synthetic phospholipid vesicles and submitochondrial particles during osmotic swelling, Biochemistry, 25 (1986) 8220-8229.

[29] C.A. Rutkowski, L.M. Williams, T.H. Haines, H.Z. Cummins, The elasticity of synthetic phospholipid vesicles obtained by photon correlation spectroscopy, Biochemistry, 30 (1991) 5688-5696.

[30] W. Chen, J. Du, Ultrasound and pH Dually Responsive Polymer Vesicles for Anticancer Drug Delivery, Sci. Rep., 3 (2013).

[31] H. Xu, Y.-H. Deng, K.-Q. Wang, D.-W. Chen, Preparation and Characterization of Stable pH-Sensitive Vesicles Composed of α-Tocopherol Hemisuccinate, AAPS PharmSciTech, 13 (2012) 1377-1385.

[32] J. Du, S.P. Armes, pH-Responsive Vesicles Based on a Hydrolytically Self-Cross-Linkable Copolymer, Journal of the American Chemical Society, 127 (2005) 12800-12801.

[33] C. Kirby, G. Gregoriadis, Dehydration-Rehydration Vesicles: A Simple Method for High Yield Drug Entrapment in Liposomes, Nat Biotech, 2 (1984) 979-984.

[34] T.F. Zhu, J.W. Szostak, Preparation of large monodisperse vesicles, PloS one, 4 (2009) e5009.

[35] D. Demirgoz, T.O. Pangburn, K.P. Davis, S. Lee, F.S. Bates, E. Kokkoli, PR_b-targeted delivery of tumor necrosis factor-[small alpha] by polymersomes for the treatment of prostate cancer, Soft Matter, 5 (2009) 2011-2019.

[36] M.N. Rhyner, The Coulter principle for analysis of subvisible particles in protein formulations, The AAPS journal, 13 (2011) 54-58.

[37] O.A. Saleh, L.L. Sohn, Quantitative sensing of nanoscale colloids using a microchip Coulter counter, Review of Scientific Instruments, 72 (2001) 4449-4451.

[38] M. Koch, A.G.R. Evans, A. Brunnschweiler, Design and fabrication of a micromachined Coulter counter, Journal of Micromechanics and Microengineering, 9 (1999) 159.

[39] Y. Rudzevich, Y. Lin, A. Wearne, A. Ordonez, O. Lupan, L. Chow, Characterization of liposomes and silica nanoparticles using resistive pulse method, Colloids and Surfaces A: Physicochemical and Engineering Aspects, 448 (2014) 9-15.

[40] R.W. DeBlois, C.P. Bean, Counting and Sizing of Submicron Particles by the Resistive Pulse Technique, Review of Scientific Instruments, 41 (1970) 909-916.

[41] L.J. Steinbock, G. Stober, U.F. Keyser, Sensing DNA-coatings of microparticles using micropipettes, Biosensors and Bioelectronics, 24 (2009) 2423-2427.

[42] W. Gao, D. Vecchio, J. Li, J. Zhu, Q. Zhang, V. Fu, J. Li, S. Thamphiwatana, D. Lu, L. Zhang, Hydrogel Containing Nanoparticle-Stabilized Liposomes for Topical Antimicrobial Delivery, ACS Nano, 8 (2014) 2900-2907.

[43] W.W. Sułkowski, D. Pentak, K. Nowak, A. Sułkowska, The influence of temperature, cholesterol content and pH on liposome stability, Journal of Molecular Structure, 744–747 (2005) 737-747.

[44] I.M. Hafez, S. Ansell, P.R. Cullis, Tunable pH-sensitive liposomes composed of mixtures of cationic and anionic lipids, Biophys J, 79 (2000) 1438-1446.

[45] X. Guo, J.A. MacKay, F.C. Szoka, Jr., Mechanism of pH-triggered collapse of phosphatidylethanolamine liposomes stabilized by an ortho ester polyethyleneglycol lipid, Biophys J, 84 (2003) 1784-1795.

[46] A.-F. Bitbol, N. Puff, Y. Sakuma, M. Imai, J.-B. Fournier, M.I. Angelova, Lipid membrane deformation in response to a local pH modification: theory and experiments, Soft Matter, 8 (2012) 6073-6082.

[47] X. Zhang, S. Rehm, M.M. Safont-Sempere, F. Würthner, Vesicular perylene dye nanocapsules as supramolecular fluorescent pH sensor systems, Nat Chem, 1 (2009) 623-629.

[48] E. Feitosa, G. Karlsson, K. Edwards, Unilamellar vesicles obtained by simply mixing dioctadecyldimethylammonium chloride and bromide with water, Chemistry and physics of lipids, 140 (2006) 66-74.

[49] H. Zhu, J. Fan, Q. Xu, H. Li, J. Wang, P. Gao, X. Peng, Imaging of lysosomal pH changes with a fluorescent sensor containing a novel lysosome-locating group, Chemical communications (Cambridge, England), 48 (2012) 11766-11768.

[50] D. Andelman, Chapter 12 Electrostatic properties of membranes: The poisson-boltzmann theory, in: R. Lipowsky, E. Sackmann (Eds.) Handbook of Biological Physics, North-Holland1995, pp. 603-642.

[51] M.P. Goertz, N. Goyal, G.A. Montano, B.C. Bunker, Lipid Bilayer Reorganization under Extreme pH Conditions, Langmuir, 27 (2011) 5481-5491.

[52] R. Zimmermann, D. Kuttner, L. Renner, M. Kaufmann, J. Zitzmann, M. Muller, C. Werner, Charging and structure of zwitterionic supported bilayer lipid membranes studied by streaming current measurements, fluorescence microscopy, and attenuated total reflection Fourier transform infrared spectroscopy, Biointerphases, 4 (2009) 1-6.

[53] G. Cevc, Phospholipids Handbook, in: G. Cevc (Ed.) Chapter 18 Solute Transport Across Bilayers, Marcel Dekker, New York, 1993, pp. 639-662.

[54] J.N. Israelachvili, 7 - Repulsive Steric Forces, Total Intermolecular Pair Potentials, and Liquid Structure, in: J.N. Israelachvili (Ed.) Intermolecular and Surface Forces (Third Edition), Academic Press, San Diego, 2011, pp. 133-149.

[55] T. Tanaka, M. Yamazaki, Membrane Fusion of Giant Unilamellar Vesicles of Neutral Phospholipid Membranes Induced by La3+, Langmuir, 20 (2004) 5160-5164.

[56] G. Lei, R.C. MacDonald, Lipid Bilayer Vesicle Fusion: Intermediates Captured by High-Speed Microfluorescence Spectroscopy, Biophysical Journal, 85 (2003) 1585-1599.

[57] S.J. Marrink, A.E. Mark, The Mechanism of Vesicle Fusion as Revealed by Molecular Dynamics Simulations, Journal of the American Chemical Society, 125 (2003) 11144-11145.

[58] C.K. Haluska, K.A. Riske, V. Marchi-Artzner, J.-M. Lehn, R. Lipowsky, R. Dimova, Time scales of membrane fusion revealed by direct imaging of vesicle fusion with high temporal resolution, Proceedings of the National Academy of Sciences, 103 (2006) 15841-15846.

[59] L. Zhang, S. Granick, How to Stabilize Phospholipid Liposomes (Using Nanoparticles), Nano Letters, 6 (2006) 694-698.

[60] Y. Yu, S.M. Anthony, L. Zhang, S.C. Bae, S. Granick, Cationic Nanoparticles Stabilize Zwitterionic Liposomes Better than Anionic Ones, The Journal of Physical Chemistry C, 111 (2007) 8233-8236.

[61] D. Pornpattananangkul, L. Zhang, S. Olson, S. Aryal, M. Obonyo, K. Vecchio, C.-M. Huang, L. Zhang, Bacterial Toxin-Triggered Drug Release from Gold Nanoparticle-Stabilized Liposomes for the Treatment of Bacterial Infection, Journal of the American Chemical Society, 133 (2011) 4132-4139.

[62] M. Kokkona, P. Kallinteri, D. Fatouros, S.G. Antimisiaris, Stability of SUV liposomes in the presence of cholate salts and pancreatic lipases: effect of lipid composition, European Journal of Pharmaceutical Sciences, 9 (2000) 245-252.

[63] H. Takeuchi, H. Yamamoto, T. Toyoda, H. Toyobuku, T. Hino, Y. Kawashima, Physical stability of size controlled small unilameller liposomes coated with a modified polyvinyl alcohol, International Journal of Pharmaceutics, 164 (1998) 103-111.

[64] R.A. García, S.P. Pantazatos, D.P. Pantazatos, R.C. MacDonald, Cholesterol stabilizes hemifused phospholipid bilayer vesicles, Biochimica et Biophysica Acta (BBA) - Biomembranes, 1511 (2001) 264-270.